3-3 Mineralization in the Eastern Area

In the eastern part of the surveyed area, the remarkable indications of mineralization are distributed in the alternation zone composed mainly of acidic volcanic rocks and tuffaceous mudstone, which is correlated with the succession of the horizon of the Hajar ore deposit. Among them, the most remarkable ones are recognized at the northeast of the Oukhribane block and in the Amzourh block. The assay results of the samples collected from the main mineralized and altered zones are as follows.

Locality	Sample No.	Cu (%)	Pb (%)	Zn (%)
Oukhribane	No.327	1.08	0.92	1.52
Oukhribane	No.335	0.66	0.12	0.12
Amzourh	No.311	0.03	0.06	1.88
Amzourh	No.314	4.40	8.40	0.26

The sample No.327 was collected at about 0.4 km northwest of Oukhribane and the sample No.335 was collected at about 1 km northwest of Oukhribane. They are gossans accompanied with network quartz vein. The sizes of the gossans are 80 m x 50 m and 30 m x 20 m, respectively. They are distributed near along the boundary zone between the tuffaceous mudstone and the alternation of sandstone and slate.

The sample No.311 was collected from the gossan contained in the acidic volcanic rock, and the sample No.314 was collected from the gossan distributed in the fracture zone found in the alternation of siltstone and slate.

In the Tiferouine area about 3 km south of Oukhribane, although the surface is covered with the Quaternary sediments, a remarkable bipole magnetic anomaly has been confirmed, the intensity of which is after that in the Hajar area. Diamond drilling of three holes, total length of which is 1,300 meters, was carried out targetting the above magnetic anomaly. However, the result has been no more than the confirmation of pyrrhotite dissemination and magnetite veinlets in the basement green rocks at the depth of about 90 meters. Further exploration is warranted in this area.

3-4 Mineralization in the Western Area

(1) Frizem Mineralization Zone

In the Frizem area, rhyolitic rocks are distributed and a high magnetic anomaly corresponding to the rhyolite has been confirmed. In the pelitic schist underlying the rhyolite, many gossans are recognized to be seated. The gossans are discontinuously distributed, associated with the bedding faults of NNW system. The gossans located in the Frizem village and at about 1 km west of the village are worth noted.

The area of distribution of the gossan in the east has the width of 80 m in maximum and is extending more than 600 meters, while that of the gossan in the west has the width of several meters in maximum and is extending about 1.5 km.

These gossans are composed mainly of siderite, hematite and quartz, and green copper dissemination is recognized. The assay result of the gossans is as follows.

Locality	Sample No.	Cu (%)	Pb (%)	Zn (%)
Frizem East	No.188	7.00	5.25	5.80
Frizem East	No.191	0.36	6.90	2.58
Frizem West	No.194	4.50	0.29	8.40
Frizem West	No.196	4.80	3.20	0.96

Diamond drilling of 10 holes was carried out for the potentiality at the depth of the gossan in the east, and the existence of low grade disseminated ore and network ore has been confirmed. The main ore minerals are pyrite, pyrrhotite and chalcopyrite which are associated with galena and sphalerite. Gangue minerals are mainly quartz, calcite and chlorite. Compared with the mineral composition of the Hajar ore deposit, it is characteristic that pyrite and copper minerals are more frequently contained in this indication of mineralization, which is thought to be suggestive of the predominance of vein type mineralization in this area. The Frizem mineralization zone shows a tendency to become predominant toward southeast, where it is covered with the Quaternary sediments.

Quartz veins of this area are estimated to have been formed in the ocean floor, judging from the evidence that the quartz grains are extensively fractured and brecciated and existed with gossaneous dusty materials.

(2) Other Indication of Mineralization

Galena-quartz vein at about 4 km west of Frizem:

Strike ; N45°W, Dip ; 50°N,

Width of galena-disseminated vein ; approx. 5 cm

Assay result ; Ag 14.0 g/t, Cu 0.04 %, Pb 1.65 %, Zn 2.28 %

Quartz vein associated with gossan about 1.5 km east of Taouililt :

Strike ; N70°W, Dip ; 70°N, Width of vein ; 2.5 m,

Assay result ; Cu 1.76 %, Zn 1.75 %,

Location ; along the northern extention of the Frizem mineralization zone, at about 1.5 km north of it.

Mineralization ; Lots of quartz veins and small alteration zones are found in the surrounding area, partly associated with green copper dissemination.

Fractured manganese-oxide quartz veins about 1 km east of Guemassa:

Strike ; N70°E, Dip ; 85°S, Width of vein ; 1 m,

Strike ; N80°E, Dip ; 80°E, Width of vein ; 0.5 m

Argillization zone in and around Daoud:

The argillaceous altered zones are sporadically accompanied by quartz veins of NNE trend.

The area extends about 2 km south of Daoud.

Magnetic anomaly zone near Mjed:

In the area of 6 km in east and west and 5 km in north and south, near Mjed, a magnetic anomaly of ∞ shape has been confirmed. The area is mostly covered with the Quaternary sediments, but at a locality about 0.5 km northwest of Mjed village, two layers of limestone beds (thickness 2 m and 4 m respectively) are exposed. They have been replaced by siderite and quartz. Diamond drilling of 1 hole was carried out in this area and pyrrhotite dissemination was confirmed. Further exploration is necessary.

High magnetic anomalies about 2 km and 5 km southeast of Daoud:

The surface is completely covered with the Quaternary sediments in this area and it is necessary to examine and investigate these magnetic anomalies.

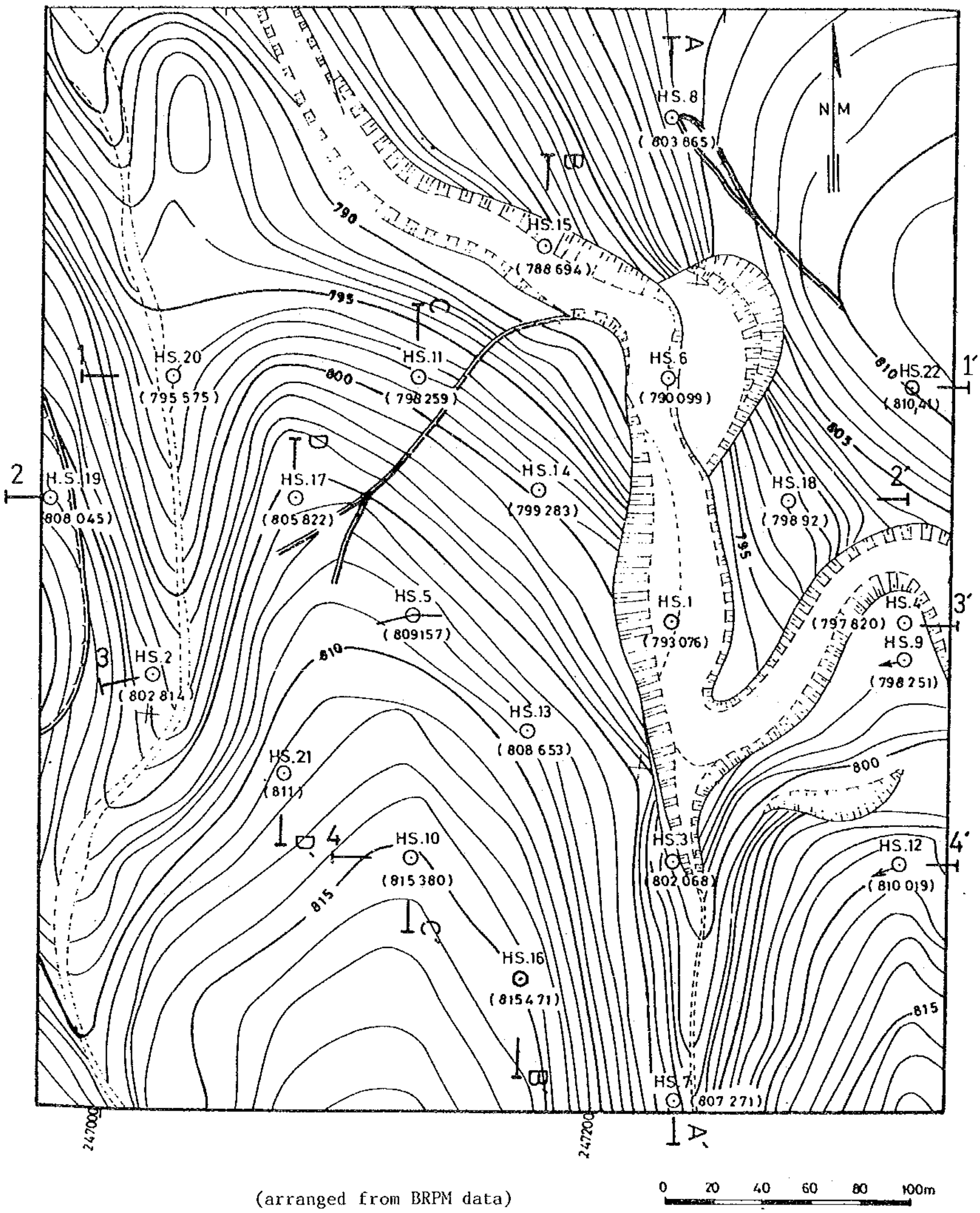

(arranged from BRPM data)

Fig. I-7 Exploration Map of Hajar Mine (1) Drilling Site

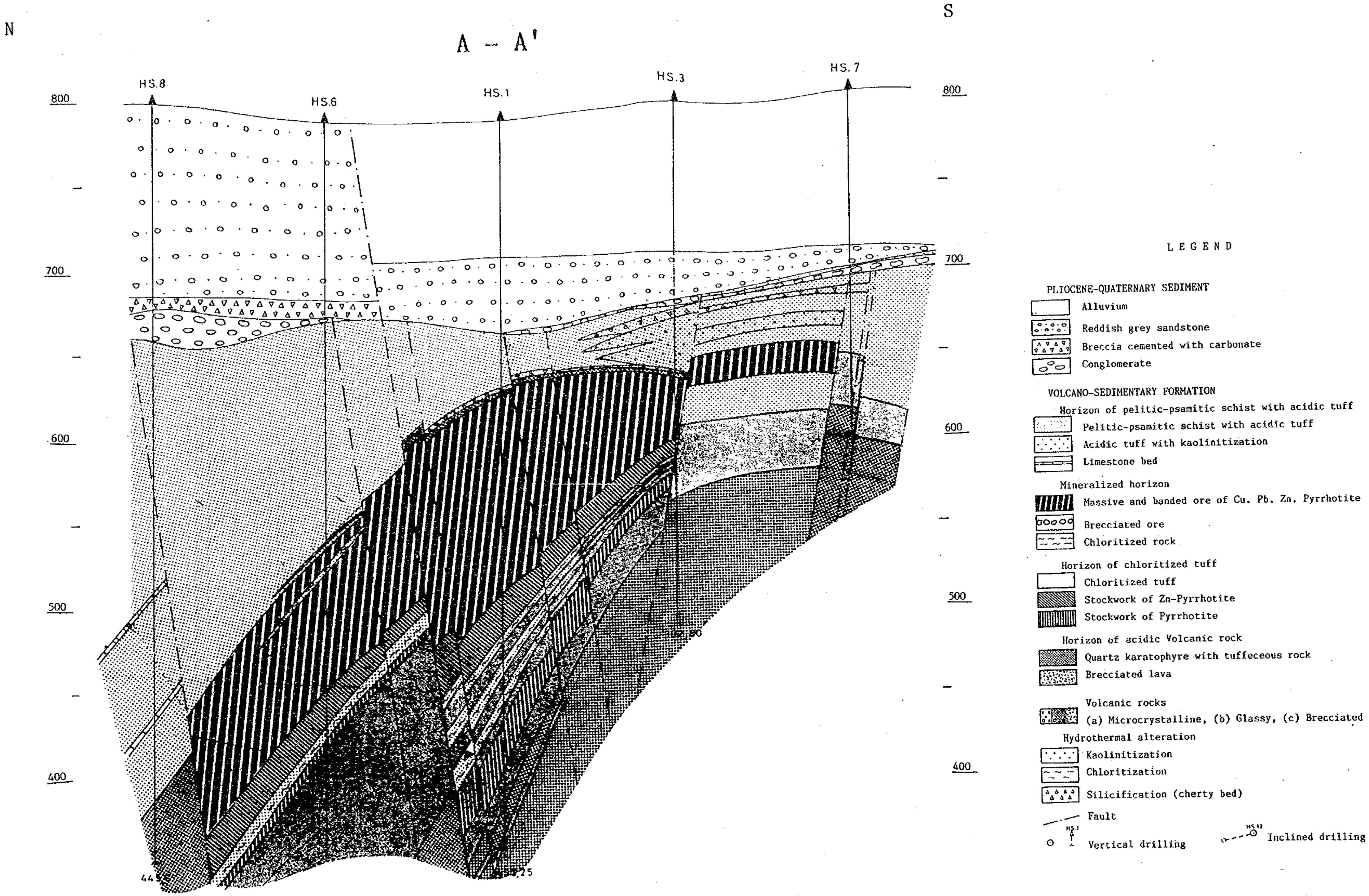

Fig. I-7 (2) A-A' Section

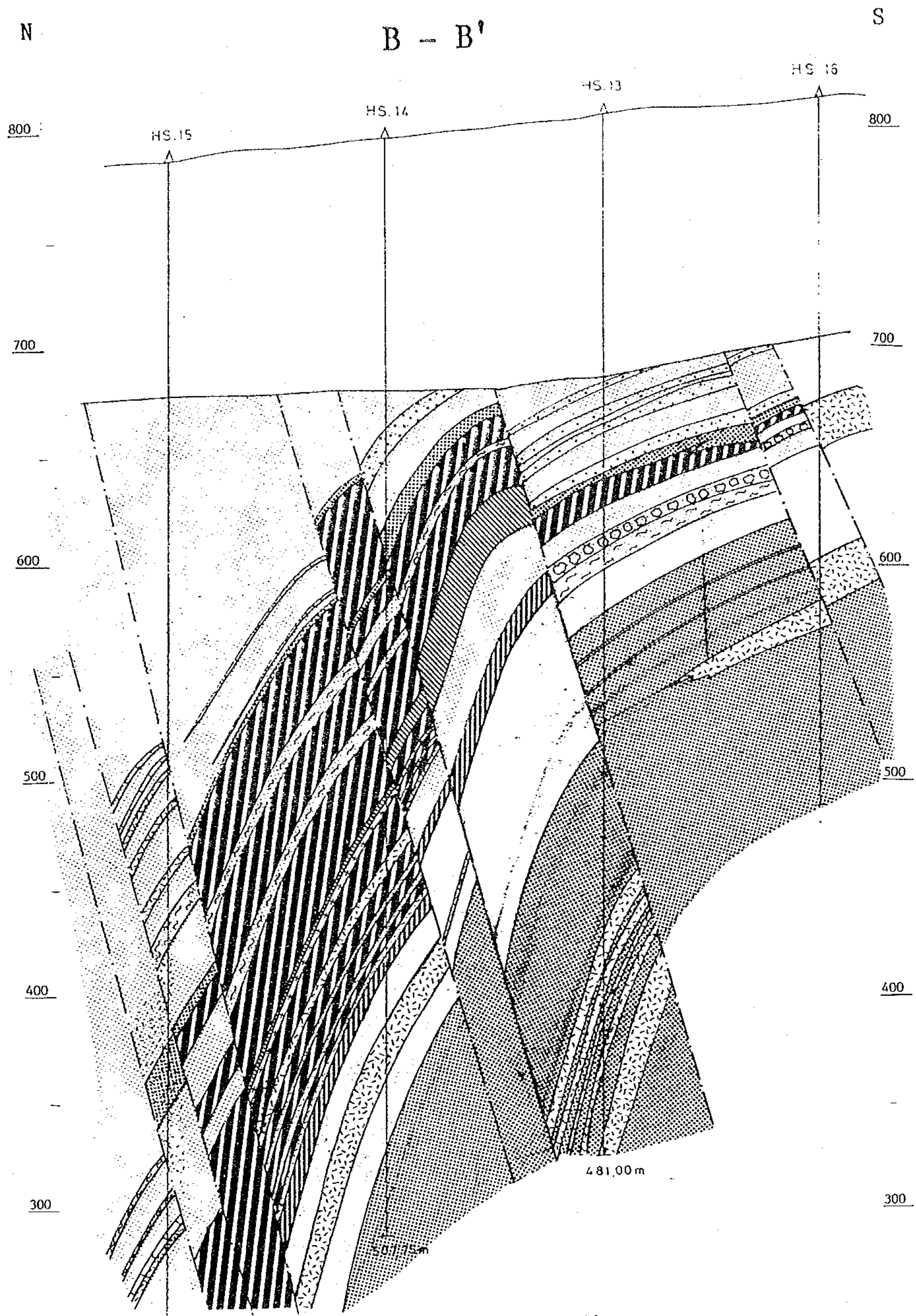

Fig. I-7 (3) B-B' Section

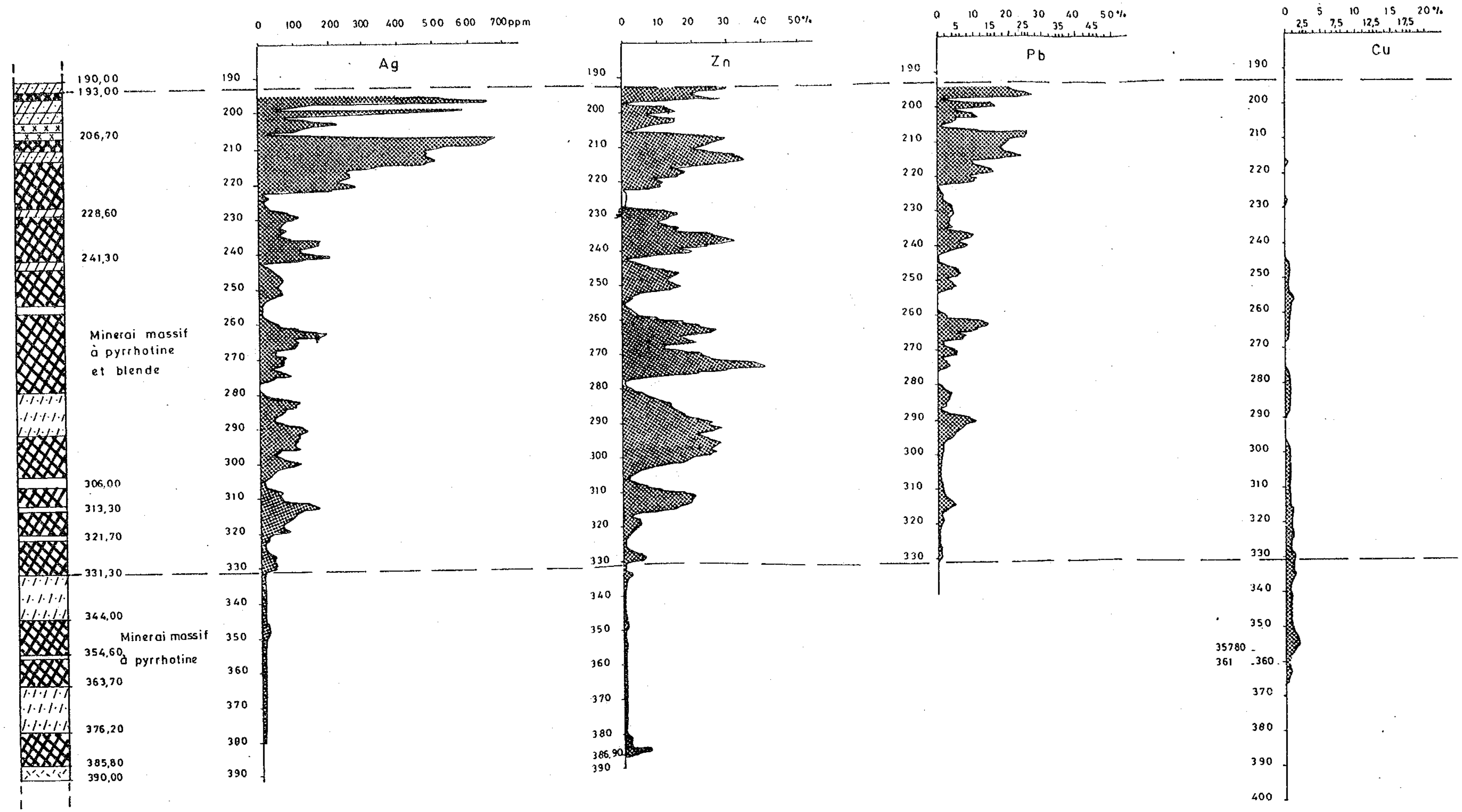

Fig. I-7 (4) Grade Distribution (HS-14)

CHAPTER 4 GEOCHEMICAL SURVEY

4-1 Outline of the Geochemical Survey (Fig. I-8)

The following two items were taken up as target for the geochemical exploration in this area.

1) Confirmation of indications of mineralization
2) Confirmation of the degree of concentration of metal elements in each difference rock types and strata, for the analysis of the period of mineralization and its characteristics.

Total 215 samples of rocks including 13 samples of gossans were collected for the geochemical exploration. These rock samples were collected with a rock hammer, about 2 kg each in weight, and they were sent immediately to the laboratory for analysis. The geochemical analysis results are shown in the Ap. I-7.

The limit of precision for the analysis is as follows.

Ag = 0.1 ppm
Cu, Pb, Zn = 1 ppm

4-2 Statistical Analysis

The statistical analysis was carried out with computer, after gossan samples were excluded, as they belong to other population than that of ordinary rock samples.

As there are many low grade assay values, the frequency distribution of the real values has strong inclination to low grade side. For the approximation of this frequency distribution to normal distribution, logarithms of the assay values were employed here, and the geometrical mean (M) and the standard deviation (σ) was calculated. Also, histograms and cumulative frequency curves were prepared for the extraction of anomalous values. The same process of analysis was carried out with each different stratum, and the mechanism of concentration of metal element was considered.

The statistical values are given in the Tab. I-1, and the histogram and cumulative frequency curve are shown in the Fig. I-9 and I-10.

The correlation coefficients of content of the metal elements in the total of 202 rock samples excluding gossans are shown below. A positive correlation is found in the relation between Pb and Zn. Both Ag and Cu do not show any correlations to other elements.

Element	AG	CU	PB	ZN
AG	1.00000	0.07531	0.25310	0.17907
CU	0.07531	1.00000	0.05234	0.38423
PB	0.25310	0.05234	1.00000	0.70623
ZN	0.17907	0.38423	0.70623	1.00000

4-3 Geochemical Anomalies

The threshould values for the extraction of anomalous values were established as given below, on the basis of the type of frequency distribution and the degree of bending of the cumulative frequency curve, considering the value of $M + 2\sigma$.

Ag : 6.0 ppm ($M + 2\sigma = 6.0$)
Cu : 200 ppm ($M + 2\sigma = 170$)
Pb : 300 ppm ($M + 2\sigma = 229$)
Zn : 700 ppm ($M + 2\sigma = 713$)

According to the above threshould values, the numbers of anomalous values are none for Ag, 8 for Cu, 4 for Pb and 12 for Zn. Including anomalous values with gossans, the total numbers are 2 for Ag, 16 for Cu, 9 for Pb and 17 for Zn.

The geochemical anomalous values of each samples are shown in the Tab. I-2. The distribution of the anomalous values in each area is as follows.

Layers of the horizon of Hajar Ore Deposit
Oukhribane area 3 samples (Cu 2, Pb 0, Zn 1)
Amzourh area 4 samples (Cu 2, Pb 1, Zn 2)
Hajar mine 3 samples (Cu 1, Pb 3, Zn 2)
Frizem area 8 samples (Ag 2, Cu 7, Pb 3, Zn 6)
Daoud area 4 samples (Cu 1, Pb 2, Zn 2)
Other areas 4 samples (Cu 3, Zn 4)

The above distribution of the anomalous values in each area shows that the remarkable anomalous zones are concentrated in Oukhribane area, in

Frizem area and in the layers of the horizon of Hajar ore deposit including Amzourh area. The geochemical anomalies in Daoud area are generally caused by quartz veins of NNE trend. The geochemical anomalies in other areas are explained to be associated with the faulted and fractured zones of ENE trend and they are distributed in the vicinity of the Guemassa fault running to the same direction of ENE.

4-4 Metal Elements in Each Stratum (Tab. I-1)

The geometrical mean values of content of the metal elements in the total of 202 rock samples excluding gossans are Ag 6.0 ppm, Cu 27 ppm, Pb 36 ppm, and Zn 120 ppm. The geometrical mean values are thought to represent the background values in this area. The grade of concentration of the metal elements have significant variation, and the characteristic and the period of the mineralization are considered to be as follows.

(1) Volcanic Rocks in Frizem Area (Iv)

The mean values of the 3 samples are Cu 110 ppm, Pb 217 ppm, and Zn 374 ppm. Each of these Cu, Pb and Zn values shows the highest of all and the values are 3 times as high as the total average of the assay values of the whole rock samples. This is thought to be an evidence for the fact that this volcanic rocks could have some intimate relation with the Cu-Pb-Zn mineralization.

(2) Alternation Zone of the Horizon of Hajar Ore Deposit (Ia)

The average value of the 18 samples is Zn 180 ppm. This value of Zn content is the second highest after the volcanic rocks in Frizem area. However, the average values of Cu and Pb are not necessarily high. This fact is thought to suggest that the mineralization of the Hajar ore deposit is zinc-rich mineralization, whose characteristics are different from those found in the mineralization zone in Frizem, which is rich in copper and lead.

(3) Intrusive Rocks

The average values of the 4 samples are Ag 0.2 ppm, Cu 7 ppm, Pb 11 ppm and Zn 39 ppm. They are the lowest values found in this area. This is thought to show that the intrusion of these rocks occurred after the mineralization.

(4) Layers Overlying the Horizon of Hajar Ore Deposit (IIc·II_{p2})

The pelitic semischist and the carbonate semischist, which are observed to overlie the successions of the horizon of Hajar ore deposit, have Zn content of 80 ppm and 74 ppm, respectively. These values are the second lowest after those for the intrusive rocks. This is thought to be an evidence for the fact that the Hajar ore deposit can be a syngenetic ore deposit and that the deposit did not affect the overlying layers at any rate. The fact that Pb content in these two semischist are as high as 63 ppm and 64 ppm, respectively, is thought to suggest that the lead concentration could have occurred in the period of sedimentation, viewing from the point that these two rocks are dolomitic as a whole.

Tab. I — 1 Statistical Values of Geochemical Assay Results

	Classification	No.	Ag (ppm)			Cu (ppm)			Pb (ppm)			Zn (ppm)		
			Mean	M + σ	M + 2σ	Mean	M + σ	M + 2σ	Mean	M + σ	M + 2σ	Mean	M + σ	M + 2σ
	Total	202	1.32	2.81	5.96	26.8	67	170	36.0	91	229	120	292	713
0	Intrusive rock	4	0.28	0.57	1.13	7.0	11	17	11.3	17	25	40	91	211
1	Ips (Pelitic schist)	48	1.16	2.66	6.12	27.5	78	223	21.0	41	79	117	316	854
2	Iv (Volcanics)	3	1.37	4.26	13.90	110.5	524	2490	217.5	313	451	374	1519	6167
3	Ic (Carbonatic schist)	54	1.67	3.30	6.53	30.8	87	243	41.0	100	244	142	339	805
4	Ip (Pelitic schist)	37	1.27	2.34	4.33	28.5	48	82	34.9	58	98	125	175	245
5	IIp$_1$ (Pelitic semischist)	2	0.57	0.92	1.51	11.0	12	14	25.3	48	92	127	283	632
6	IIal (Alternate semischist)	18	1.44	2.59	4.65	30.4	89	263	38.6	169	737	180	580	1869
7	IIav (Volcanics)	2	1.13	1.85	3.02	11.3	18	30	27.7	34	42	83	272	887
8	IIp$_2$ (Pelitic semischist)	15	1.08	2.57	6.10	25.3	40	63	63.1	147	341	80	179	402
9	IIc' (Carbonatic semischist)	19	1.76	2.91	4.81	17.7	28	43	63.5	133	280	74	145	283

M (Mean) = Geometric mean

σ = Standard diviation

Total = excluded of gossan samples

Tab. I—2 List of Geochemical Anomalies

Area	Sample No.	Rock Type	Grade			(ppm)
			Ag	Cu	Pb	Zn
Hajar	305	Green rock	2.4	40	1120	3040
	308		2.8	150	800	1960
	309	Low-grade ore	3.6	4000	496	296
Oukhribane	325	Tuff	1.6	420	8	248
	329	Tuff	2.0	66	32	1000
	333	Gossan	1.2	440	112	116
Amzourh	311	Gossan	0.4	30	56	1880
	314	Gossan	2.4	4400	8400	256
	316	Limestone	3.6	14	220	940
	318	Gossan	3.2	620	216	272
Frizem	126	Calc sch	2.4	1760	16	1750
	135	Bndd sch	0.4	420	10	148
	184	Rhyolite	4.0	540	248	216
	188	Gossan	5.6	7000	5250	5800
	189	Pel sch	1.6	104	144	1840
	191	Gossan	10.0	360	6900	2580
	194	Gossan	8.0	4500	288	8400
	196	Gossan	5.0	4800	3200	960
Daoud	214	Calc sch	3.2	44	600	1400
	215	Calc sch	3.2	18	96	1120
	216	Calc sch	5.0	154	560	680
	218	Pel sch	1.6	420	24	84
Others	147	Psm sch	4.0	640	56	1040
	207	Pel sch	0.8	1300	120	760
	268	Pel sch	2.4	26	104	1160
	407	Pel sch	0.4	320	24	880

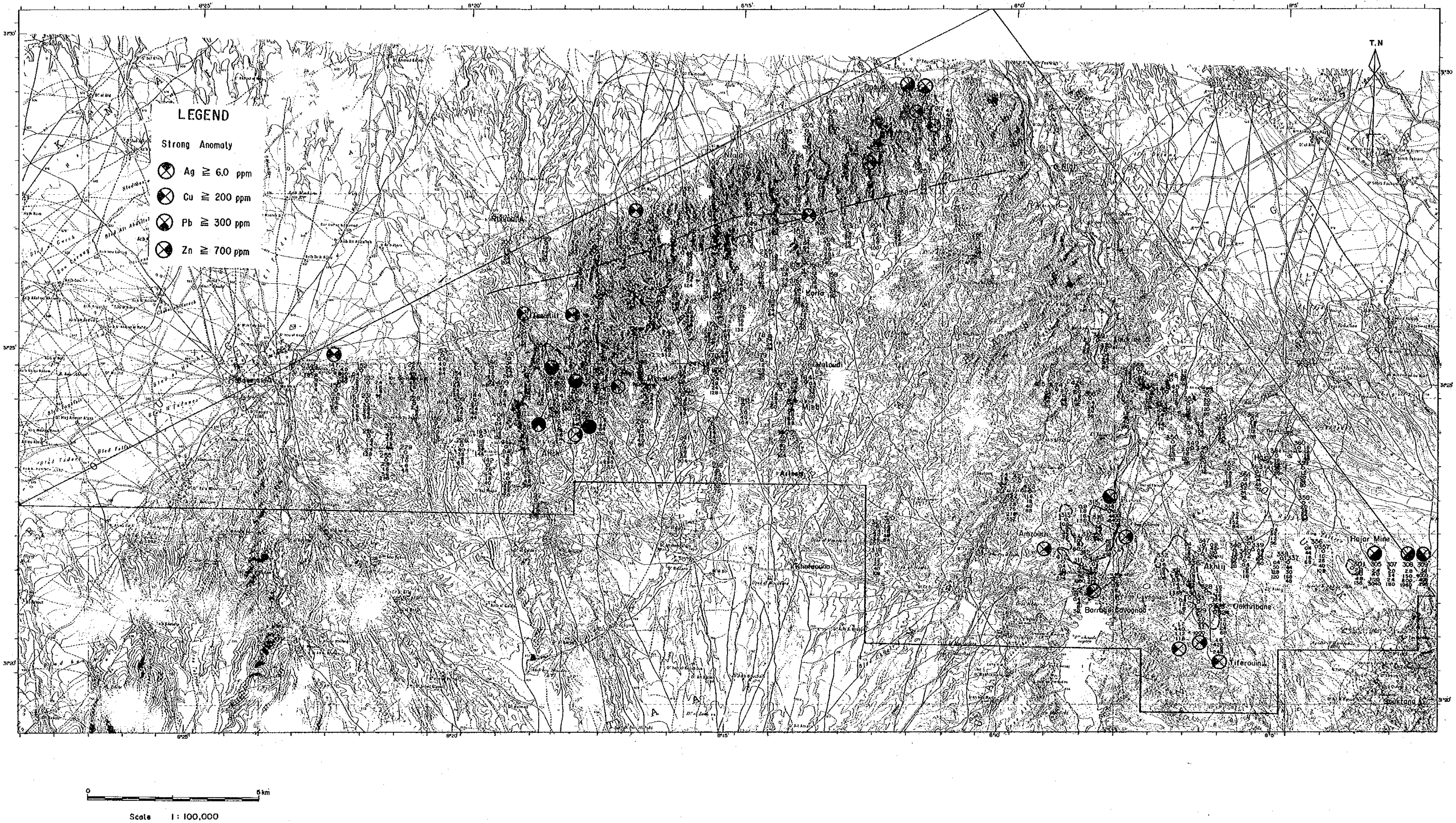

Fig. I-8 Geochemical Anomaly Map

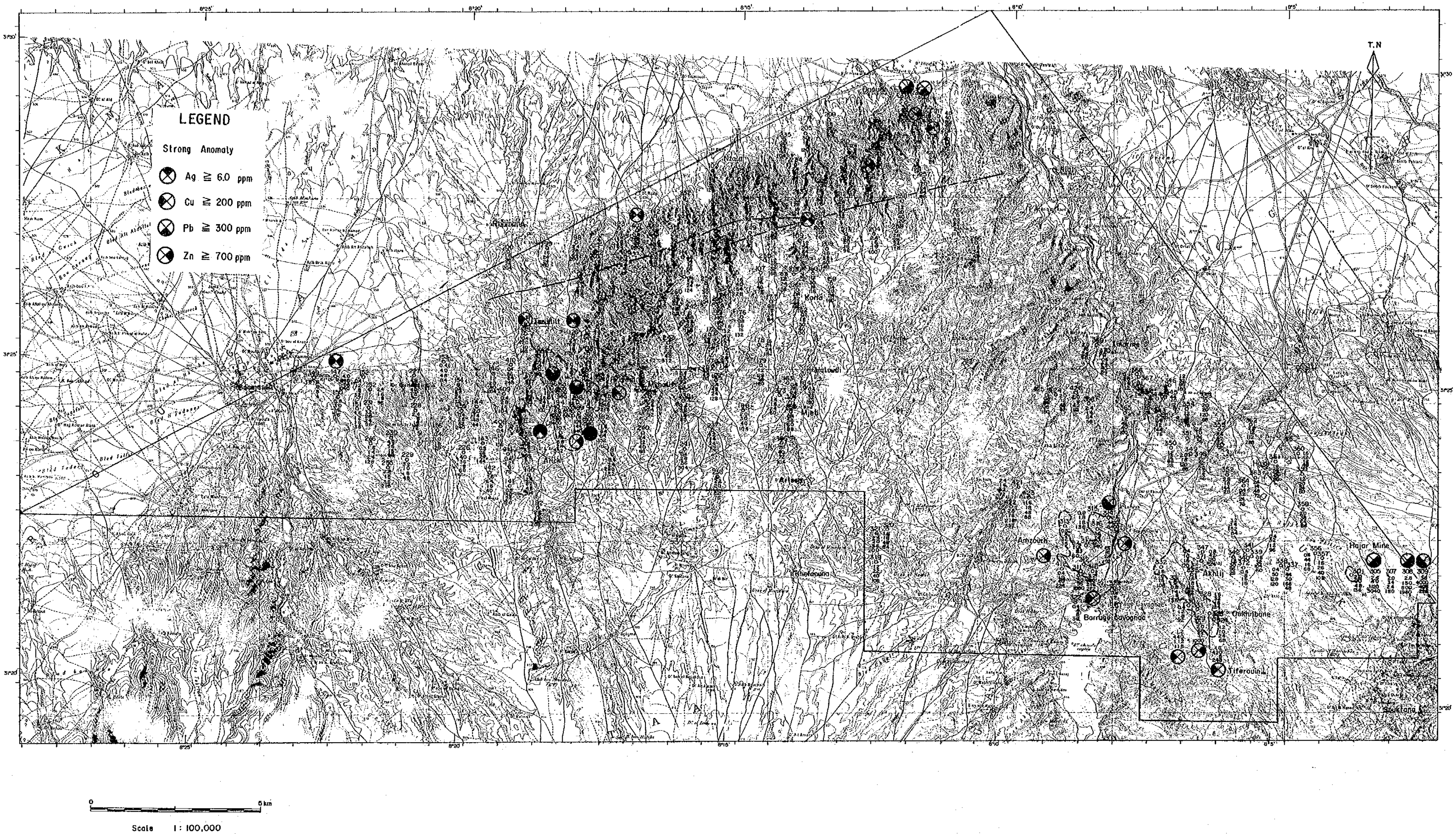

Fig. I-8 Geochemical Anomaly Map

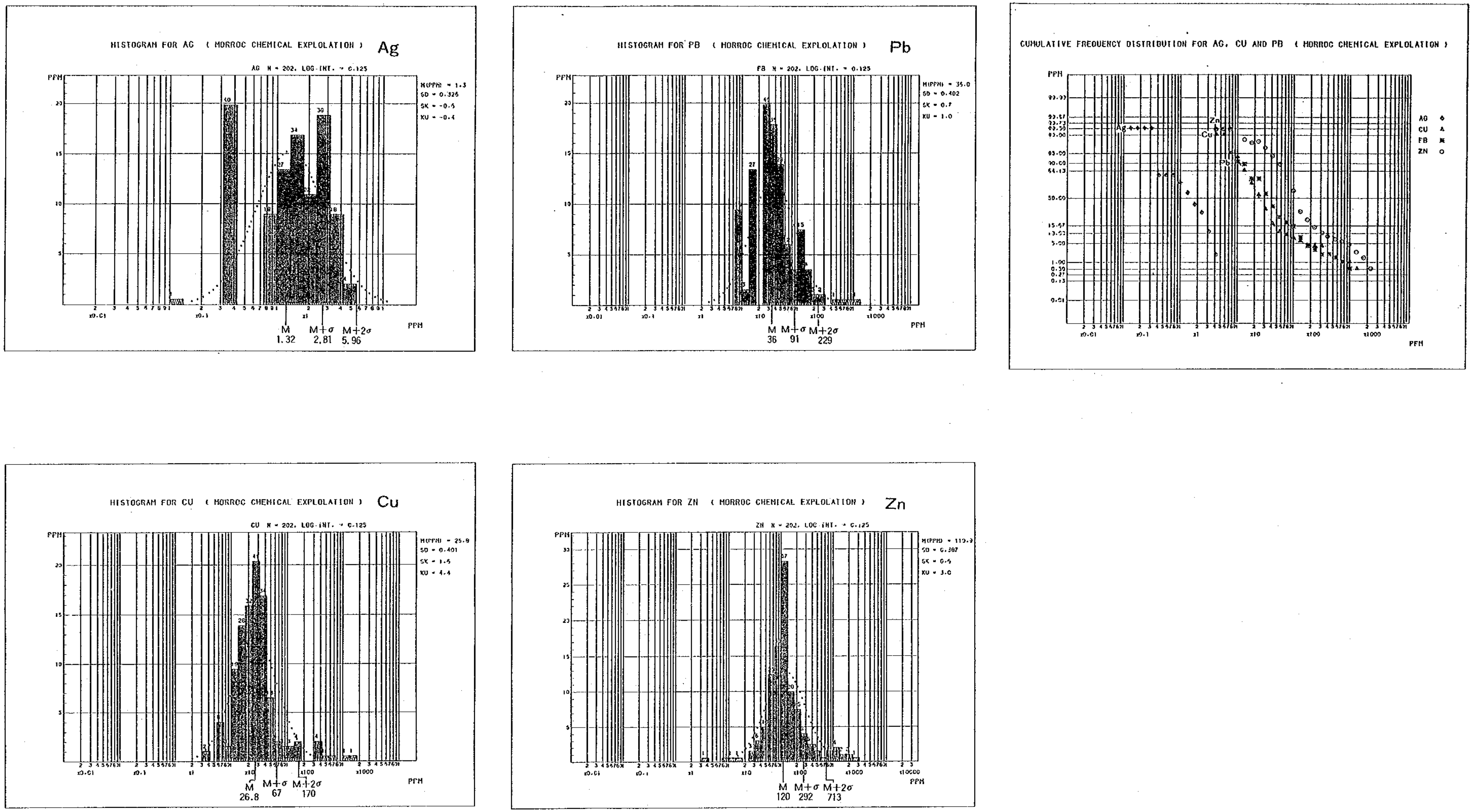

Fig. I — 9 Histogram and Cumulative Frequency Curve of Geochemical Assay Results

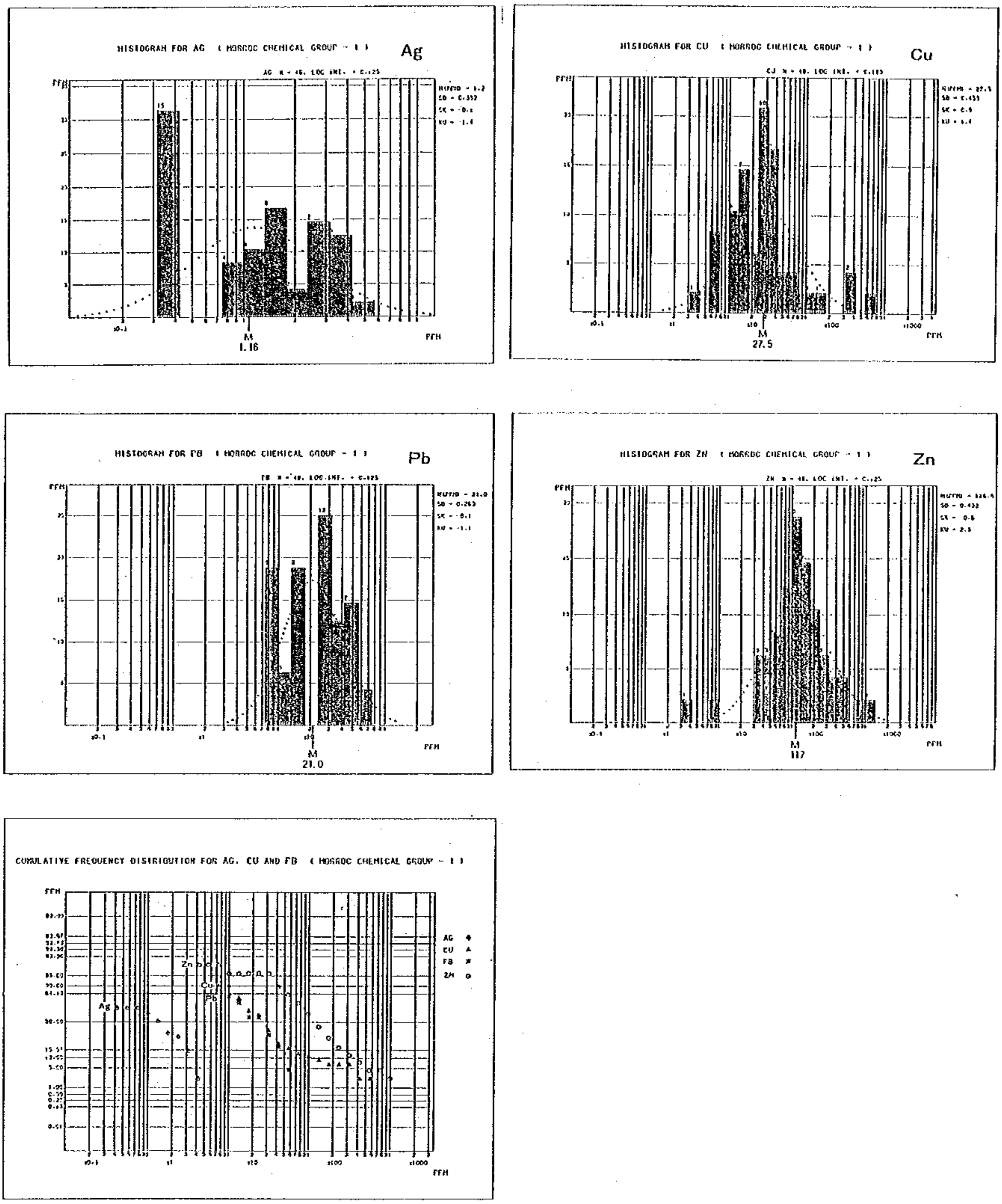

Fig. I—10 Histogram and Cumulative Frequency Curve of Geochemical Assay Results by Each Formation (1) Group I ps (Pelitic schist)

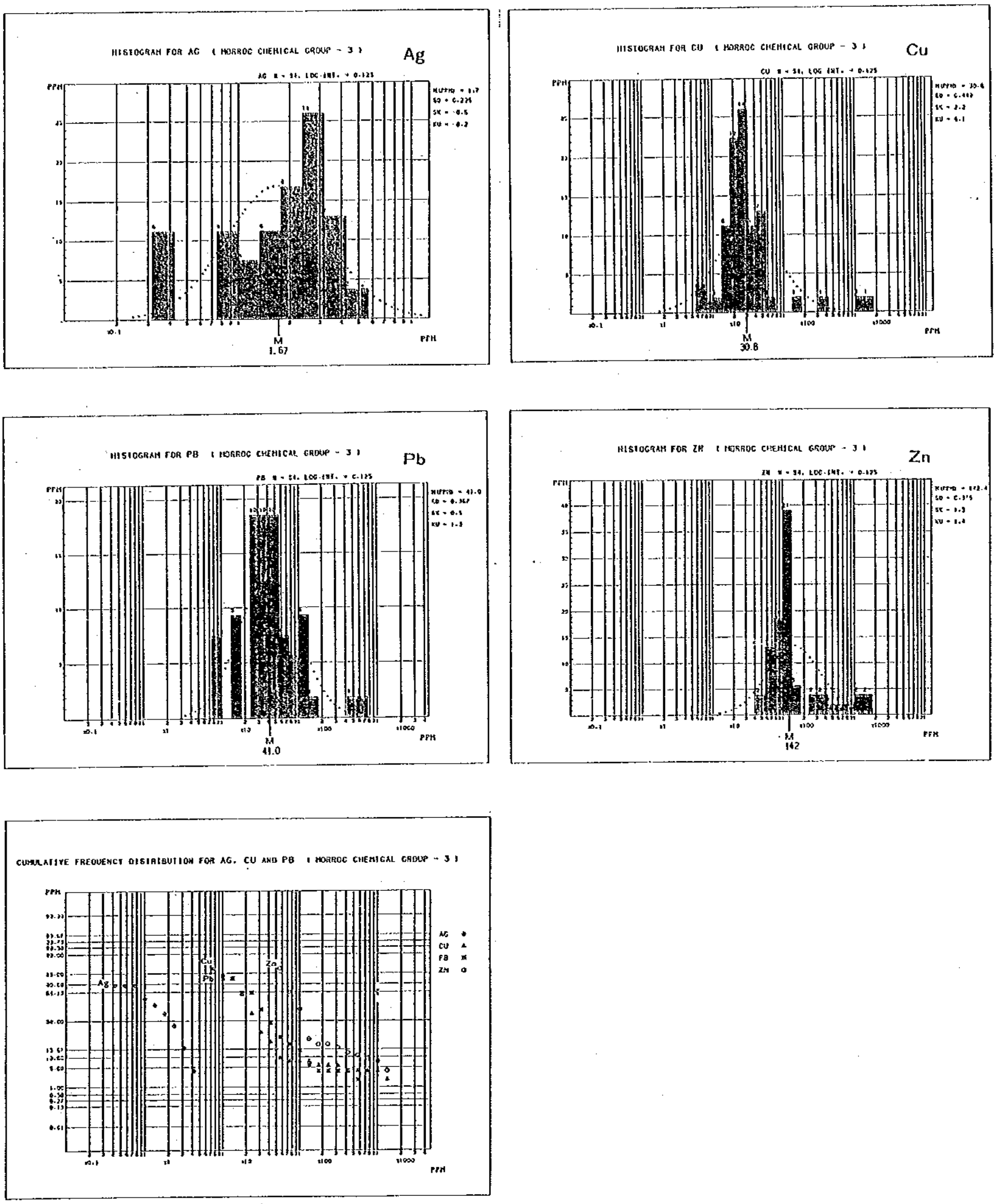

Fig. I —10 Histogram and Cumulative Frequency Curve
of Geochemical Assay Results by Each Formation
(2) Group I c (Carbonatic schist)

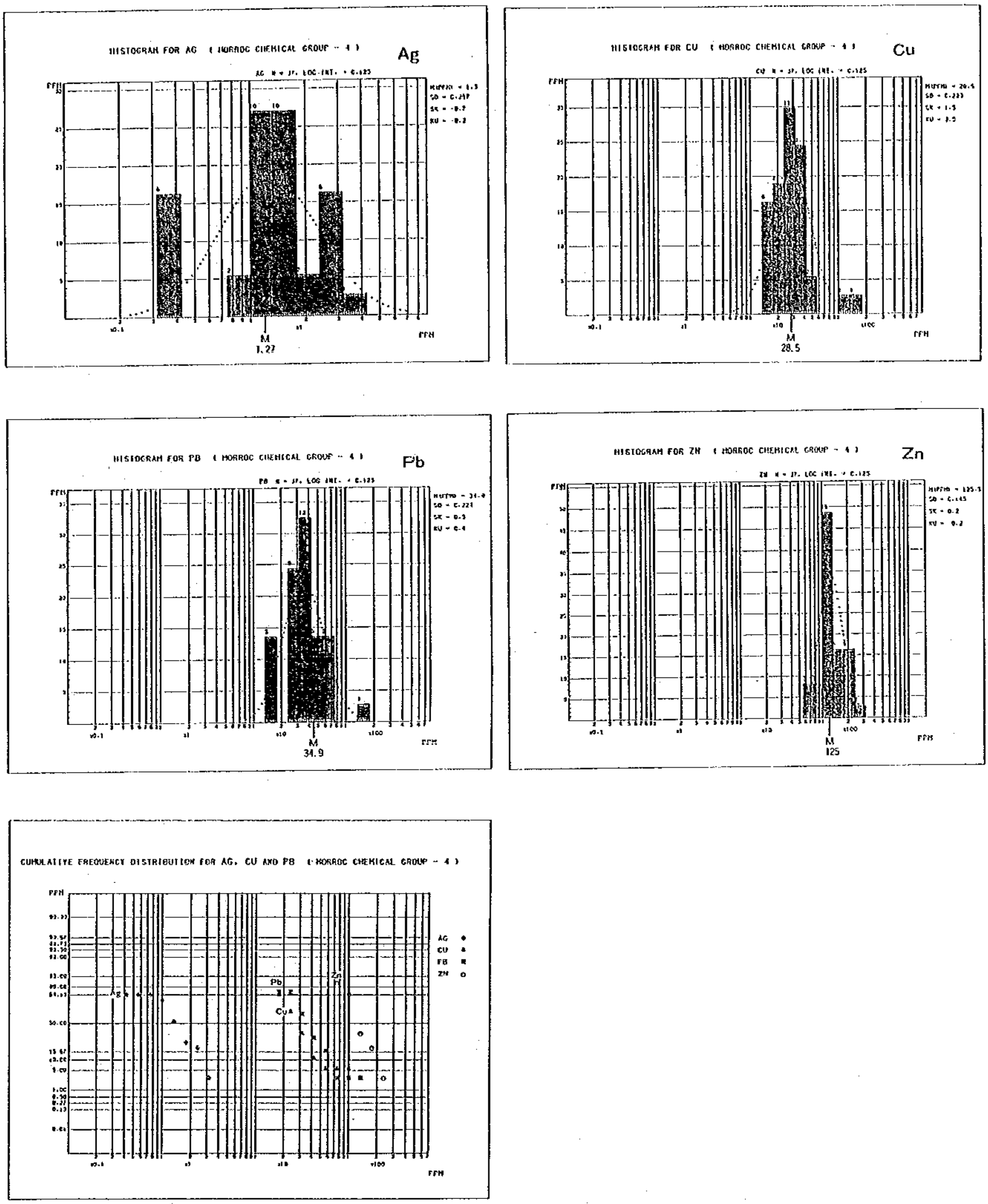

Fig. I −10 Histogram and Cumulative Frequency Curve of Geochemical Assay Results by Each Formation (3) Group I p (Pelitic schist)

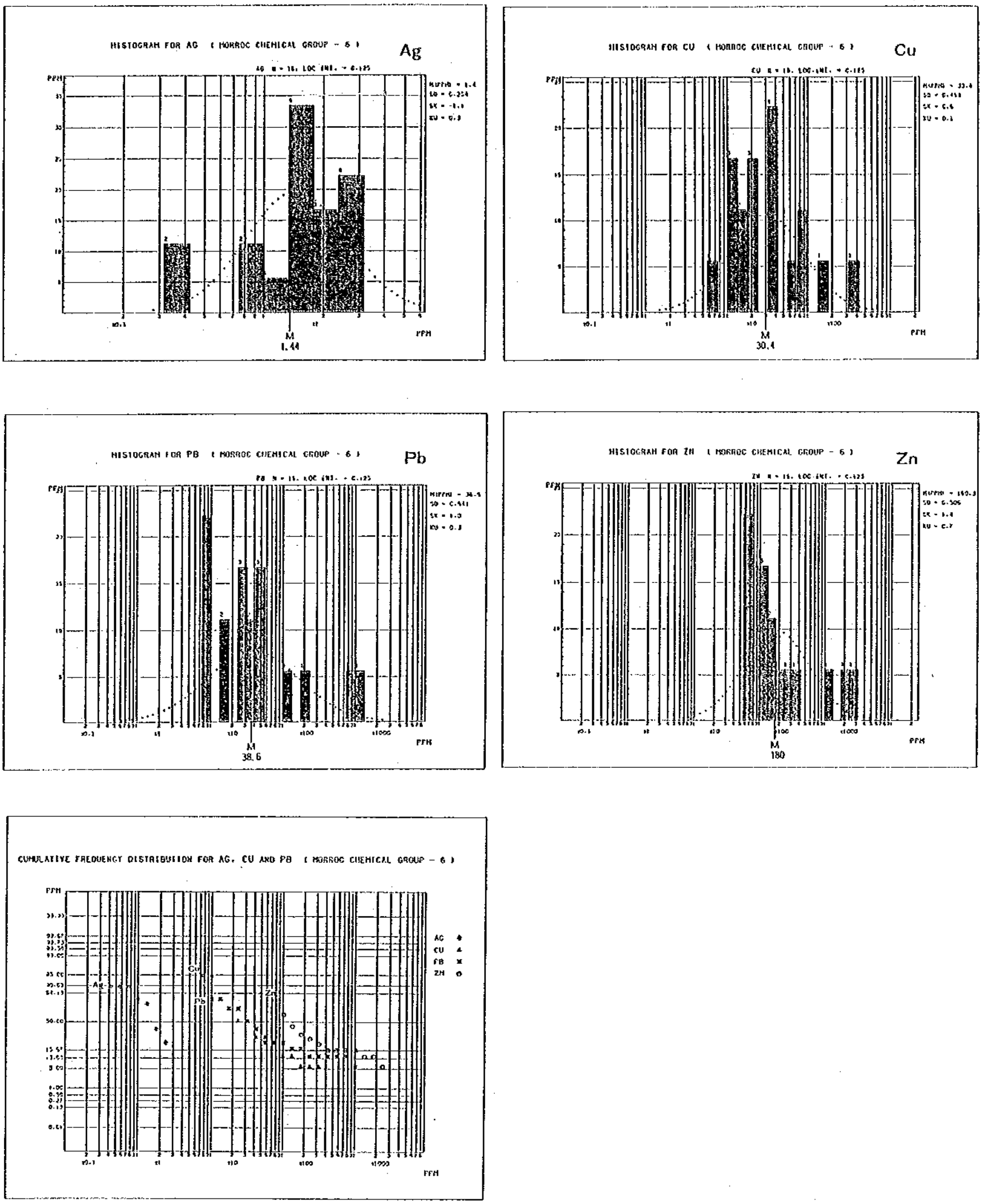

Fig. I —10 Histogram and Cumulative Frequency Carve
of Geochemical Assay Results by Each Formation
(4) Group Ⅱa (Alternate schist)

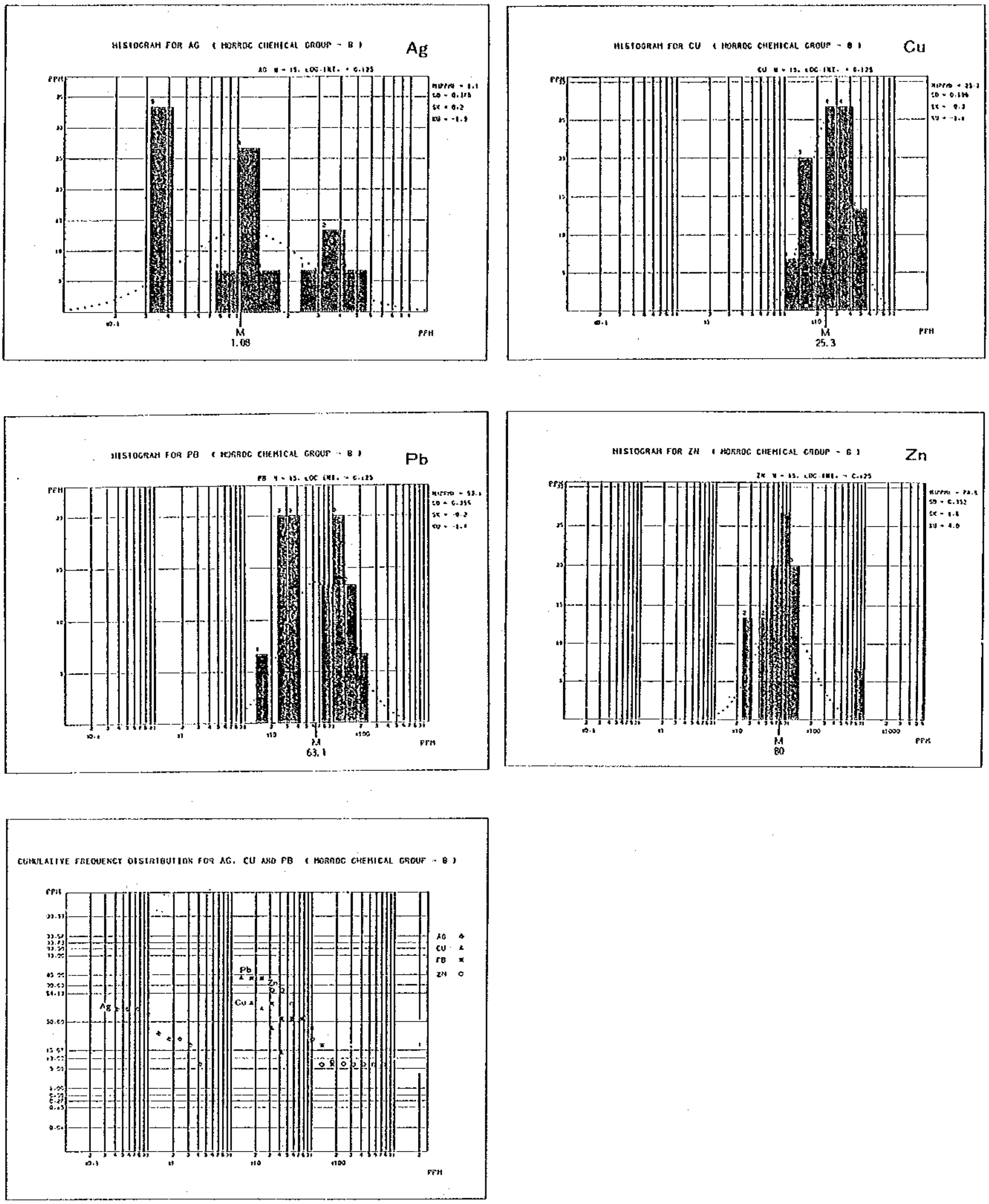

Fig. I −10 Histogram and Cumulative Frequency Curve
of Geochemical Assay Results by Each Formation
(5) Group Ⅱp2 (Pelitic schist)

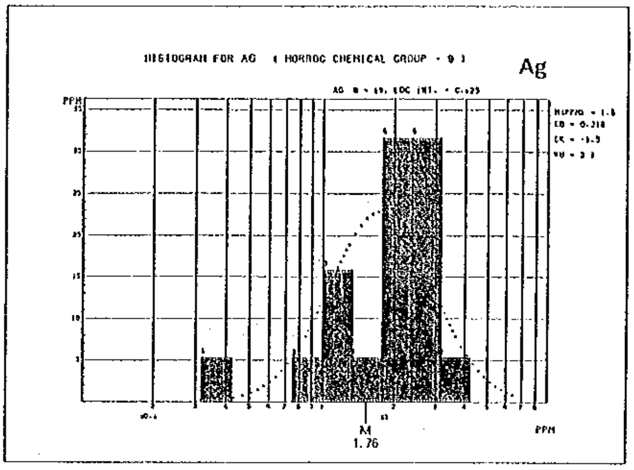

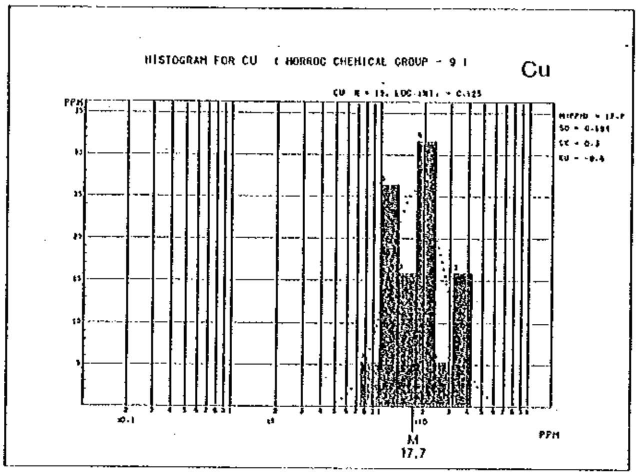

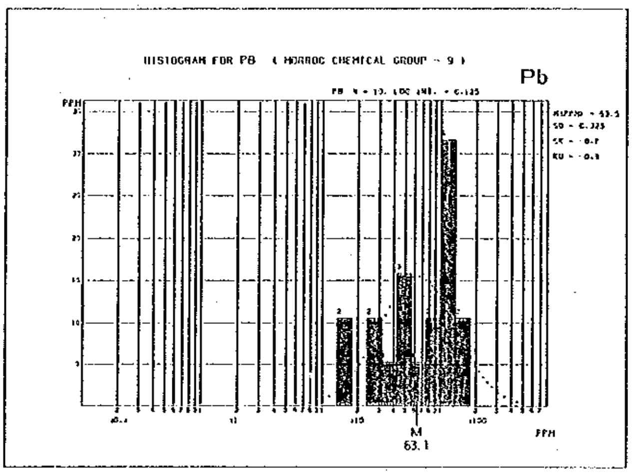

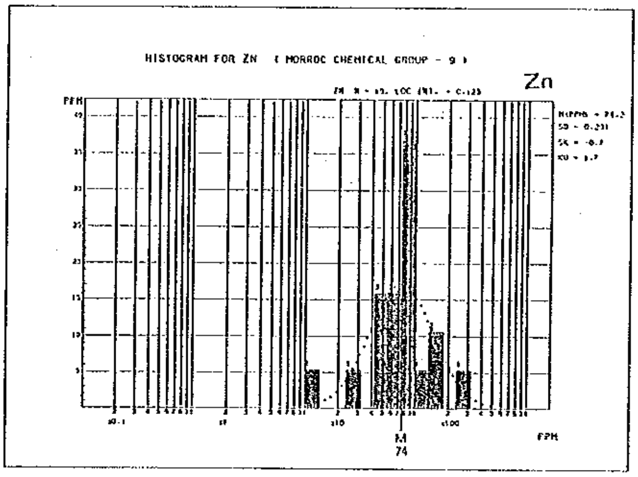

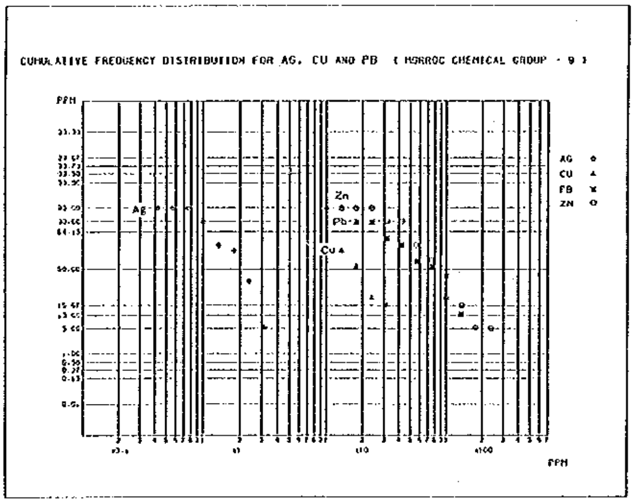

Fig. I —10 Histogram and Cumulative Frequency Curve of Geochemical Assay Results by Each Formation (6) Group II c (Carbonatic schist)

CHAPTER 5 CONSIDERATION

5-1 Geological History

The surveyed area is located geologically in the Paleozoic geosyncline which developed along the northwestern margin of the West African craton. In this geosyncline, thick upper Paleozoic sediments, composed mainly of mudstone and marl, are observed to have accumulated on the basement of the lower Paleozoic group. The upper Paleozoic group was metamorphosed by the dynamic metamorphism during the period of Hercynian orogenic movement at the end of Paleozoic or in early Mesozoic Era. The sediments such as mudstone and marl were metamorphosed to form schist and semischist constituted mainly by the minerals such as chlorite, sericite, quartz and calcite. Many drag folds, intrafolial folds and schistosity-faults are well developed, and the bedding structures of the original rocks have been deformed remarkably. A large scale syncline has been formed dipping toward the east with the axis in the direction of ENE-WSW, together with the faults in the same posture. It is estimated that, after the Alpine orogenic movement in the period of later Mesozoic or Tertiary, the land has been uplifted and eroded out to form present condition of the terrain.

5-2 Sedimentary Environment and Volcanic Activity

In the upper Paleozoic group, sediments such as mudstone and marl are found predominant, and it is thought from this viewpoint that the sedimentation of these beds occurred in a tranquil environment with little change. It might have been an inner sea surrounded by land, where some reducing environment was prevailed. The upper Paleozoic sediments are observed to contain products of at least two periods of sub-marine volcanic activity. As is recognized in the Hajar area or in the Frizem area, the sub-marine volcanic activity is represented principally by acidic volcanic rocks and pyroclastic rocks, which are thought to be suggestive of the volcanic activity to have been comparatively in small scale. It is thought that the volcanic activity would have been of the type of sub-marine fissure eruption and that this type of volcanic activity usually occurs not in such a zone as island arc where usually intense structural movement takes place, but in the extensile volcanic rift of the crust.

5-3 Characteristics of the Mineralization

The Hajar ore deposit is intimately associated with the green schist originated from acidic volcanic rocks and pyroclastic rocks. It is most characteristic that the Hajar ore deposit contains a great deal of pyrrhotite in addition to copper, lead and zinc minerals. The occurrence of pyrrhotite in the ore deposit is thought to suggest that the environment was reducing at the period of mineralization or during diagenesis. As the examples of the same type of ore deposit found in the upper Paleozoic sediments, are listed the Frizem mineralization zone where copper and lead minerals are concentrated, the Kettara ore deposit in the Jebilet mountain which contains mainly pyrrhotite associated with copper minerals, and the Rio Tinto ore deposit in the southern part of Spain in which copper minerals are concentrated although pyrite is predominant, and so on. These same type of ore deposits as the Hajar ore deposit are recognized to have been emplaced in a certain horizon of successions which are accompanied by volcanic activities, although the metal elements they contain are different with different ore deposits. It is thought to be quite important for the future exploration to elucidate comprehensively the characteristics of the volcanic activities and the structural circumstances for the emplacement of ore deposits, in addition to the pursuit of the horizon of successions where ore deposits are emplaced.

In the Frizem mineralized zone where vein type ore deposits have been confirmed presently, it needs to pursuit a possibility of the emplacement of massive sedimentary ore deposits.

In the Daoud area, it needs to clarify the exact cause of the geochemical anomalies which suggest a possibility of intrusion of igneous rock deep underground or a influence of the mineralization of Hajar ore deposit.

PARTICULARS

PART Ⅱ

GEOPHYSICAL SURVEY

CHAPTER 1 OUTLINE

1-1 Scope of the Survey

CSAMT measurements were carried out by measuring electromagnetic field generated by three transmitter bipoles (see Fig. II-1). The scope of the survey is as follows:

Area:	150 km^2
Station interval:	500m to 800m
Number of stations:	149 points from the transmitting bipole A
	76 points from the transmitting bipole B
	77 points from the transmitting bipole C
	302 points in total

Survey stations are dense in the eastern part of the survey area and not dense in the center to western part of the survey area (see PL. II-1).

1-2 Method of CSAMT Survey

The geophysical survey area is shown in Fig. II-1.

Controlled Source Audio Frequency Magnetotelluric method (called CSAMT) is a kind of magnetotelluric method with a controlled electromagnetic source. One horizontal electric field and one magnetic field, which are orthogonal to each other, are measured in ten different frequencies and apparent resistivity of each frequency is calculated.

General concept of CSAMT survey is illustrated in Fig. II-2.

Goldstein and Strangway (1975) described CSAMT method in detail.

The specifications of this CSAMT survey are as follows:

(1) Signal source

Electrode: Three pairs of electrodes were grounded in the north of the survey area.

Transmitting bipole A: 2,000m long, E-W direction

Transmitting bipole B: 1,900m long, N70°E
Transmitting bipole C: 1,800m long, E-W direction

Electrode Material: At each electrode, 8 to 11 holes (about 1m deep) were dug. Aluminum plates (0.5m * 0.5m) were buried with mixture of water, salt and bentonite in each hole.

Resistance of entire transmitting bipole system:
Transmitting bipole A: 36 ohms in the first half and 24 ohms in the last half of the survey.
Transmitting bipole B: 19 ohms
Transmitting bipole C: 37 ohms

Transmitting current: Transmitting electric current of each frequency is as follows:

Frequency (Hz)	4	8	16	32	64	128	256	512	1024	2048
Bipole A	14	14	14	14	14	14	14	12	10	7
Bipole B	12	12	12	12	12	12	12	11	9	7
Bipole C	11	11	11	11	11	11	11	11	8	4

(unit in Ampere)

(2) Signal reception
Reception mode: TE mode (potential dipole direction is parallel to general strike of geological structure).
Distance from a source bipole: Distance between a survey station and a source is over 4 km.
Potential dipole: Electrode separation is 50 m and is parallel to the direction of a transmitting bipole.
Magnetic sensor: Ferrite core coil.

Frequency: 4, 8, 16, 32, 64, 128, 256, 512, 1,024, 2,048 Hz
Recording time: Over 30 minutes.
Repetition of measurements: Measurements were repeated at least three times for each frequency at a station.

1-3 Equipment

Equipments used for the survey are manufactured by Zonge Engineering & Research Organization except an engine generator.

They are as follows:

(1) Transmitter
Engine generator (B-20, Geotronics made)
output power 30 kVA, 120/208 V, 400 Hz, 3 phases, 53 HP (at 3,600 rpm)
Transmitter (GGT-5)
maximum output 5 kw, 24A, 1,000 V
Transmitter controller (XMT-2)
frequency range: DC to 10,000 Hz

(2) Receiver
Data processor (GDP-12)
amplifier, filter, A/D converter, data processor
Antenna coil (AMT/1)
single axis ferrite core coil, sensitivity 0.2 mV/gamma Hz

1-4 Data Reduction and Analysis

Data reduction and analysis were carried out as the flow chart (see Fig. II-3).

The symbols used for this report are as follows:

ρ : true formation resistivity (Ωm)
ρa : apparent resistivity (Ωm)
$\rho a'$: apparent resistivity after near field correction (Ωm)

f	:	frequency (Hz)
Ex	:	electric field ($\mu V/m$)
Hy	:	magnetic field (nT)
d	:	skin depth (m)
r	:	distance between a transmitter bipole and a receiving station (m)
$K(r)$	:	geometric constant
h_1	:	thickness of the first layer (m)
ρ_1	:	resistivity of the first layer (Ωm)
ρ_2	:	resistivity of the second layer (Ωm)
ω	:	angular frequency ($2\pi f$)
μ	:	magnetic permeability ($4\pi \times 10^{-7} H/m$)

(1) Calculation and Average of Apparent Resistivity

Apparent resistivity, ρa, is calculated as follows:

$$\rho a = \frac{1}{5f} \left| \frac{Ex}{Hy} \right|^2 \quad \cdots\cdots\cdots\cdots\cdots\cdots \text{①}$$

Measurements were repeated for each frequency at a station and an apparent resistivity at a station of respective frequency was decided by geometrically averaging over three well-repeated field data. Apparent resistivity values are listed in Tab. II-1.

(2) Near Field Correction

Resistivity values, thus obtained, include near field effect and do not show true magnetotelluric apparent resistivity in lower frequencies, if distance between a receiving station and a transmitting bipole is near, less than three-fold of a skin depth.

$$d = 503 \sqrt{\frac{\rho}{f}} \quad \cdots\cdots\cdots\cdots\cdots\cdots\cdots\cdots\cdots\cdots \text{②}$$

Influence of near field effect is larger in resistive area. Near field effect is seen in data from all stations in the east end and the northern to western part of the survey area. Near field effect is corrected by the following equation,③, by assuming homogeneous isotropic earth.

$$\rho a' = K(r) \cdot r \cdot \left| \frac{Ex}{Hy} \right| \quad \cdots\cdots\cdots\cdots\cdots \quad ③$$

(3) Inversion

Apparent resistivity vs. frequency curves of all stations are inverted one-dimensionnaly into horizontally layered earth.

One-dimensional inversion was automatically performed as follows:

An apparent resistivity vs. frequency curve of a initial horizontally layered earth model is calculated by a computer. Then the calculated curve is compared with a field data. Usually the two has some difference. A computer looks for a more suitable horizontally layered earth model. And repeat calculation until two apparent resistivity curves match each other. Thus obtained most fitted horizontally layered earth model is one of the answers to a given field data because horizontally layered earth is assumed.

The forward equation for a two-layer earth model is as follows:

$$\rho a = \rho_1 \cdot \cot h^2 \, (c_1 h_1 + \cot h^{-1} c_1 / c_2)$$

where,

$$c_1 = \sqrt{\frac{J \omega \mu}{\rho_1}}$$

$$c_2 = \sqrt{\frac{J \omega \mu}{\rho_2}}$$

The results of one-dimensional inversion of all stations are tabulated in Ap. II-1 at the end of this report.

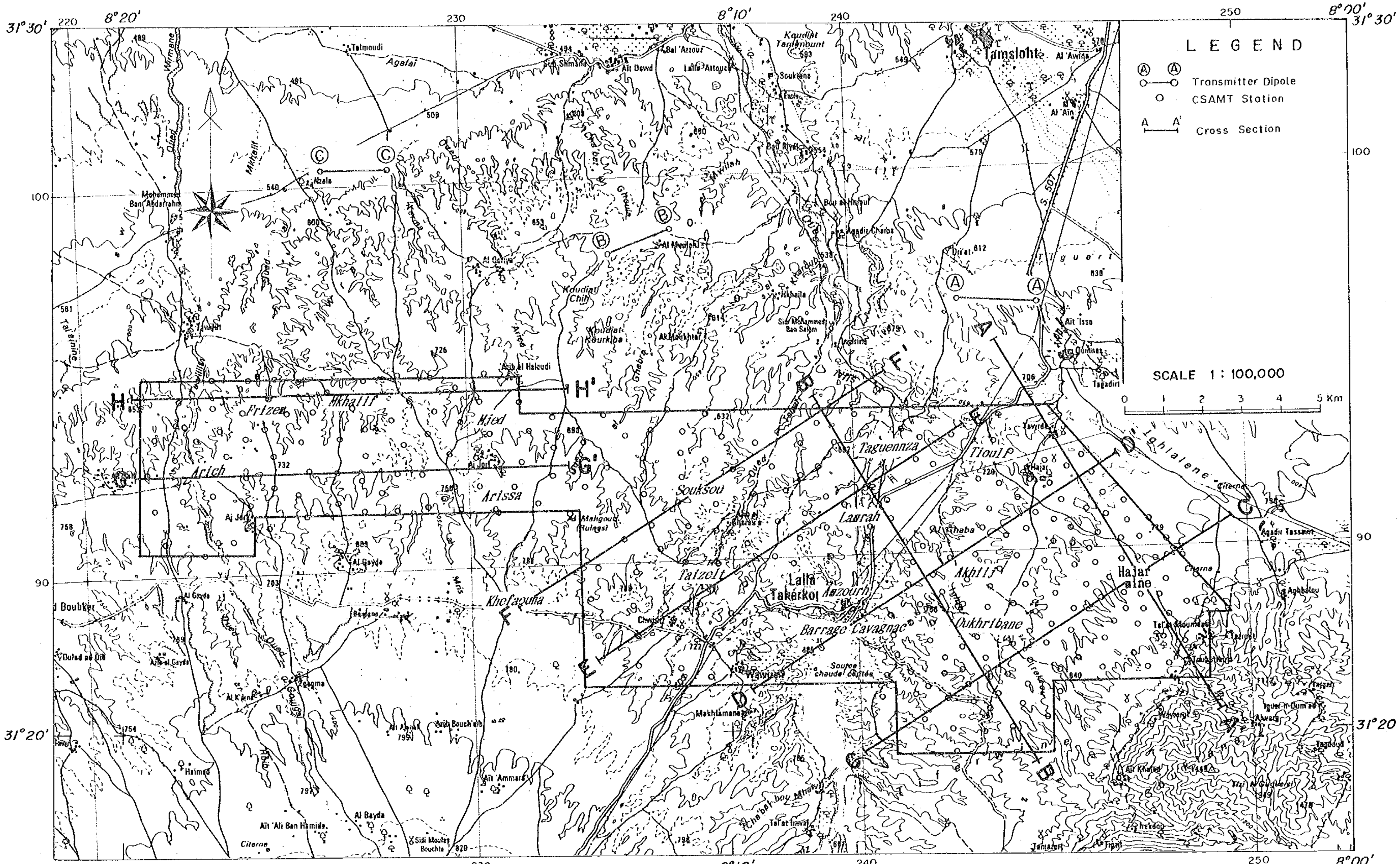

Fig. II-1 Geophysical Survey Area

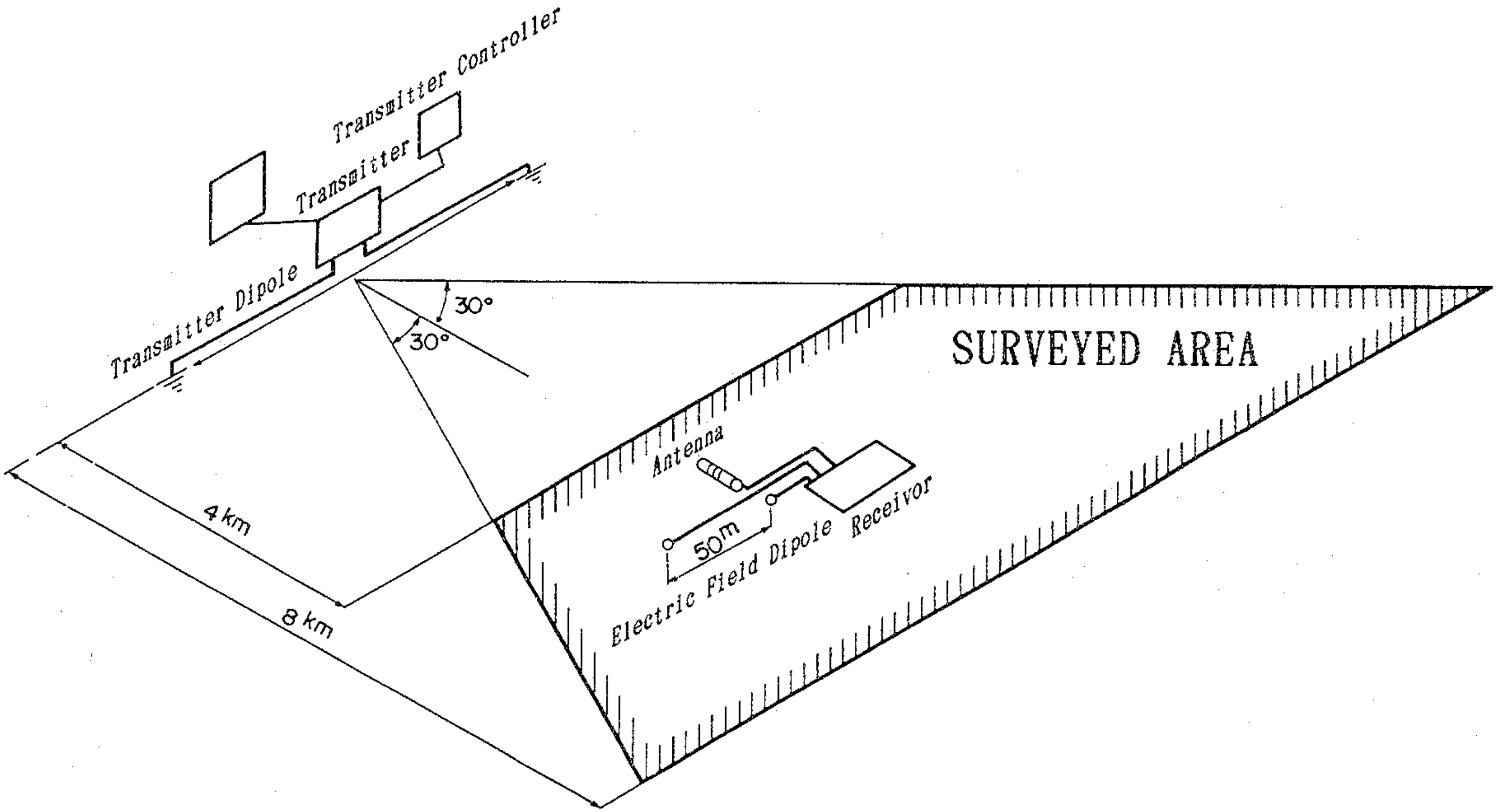

Fig. II-2 Schematic Diagram of CSAMT Survey

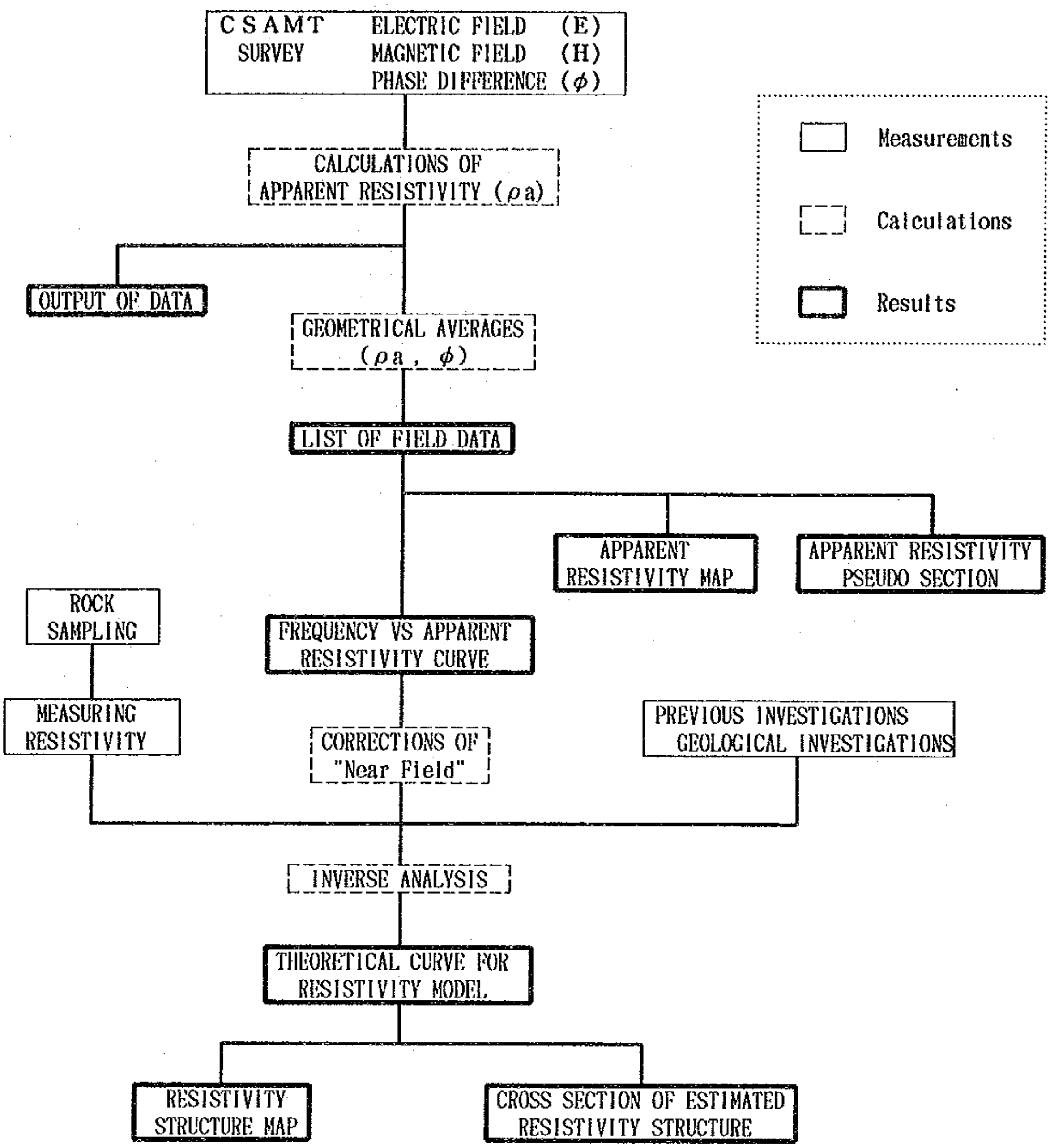

Fig. II-3 Flow Chart for CSAMT Data Processing

Tab. II-1 List of Apparent Resistivity (1/8)

ST.NO. & DIPOLE	FREQUENCIES (HZ)									
	4	8	16	32	64	128	256	512	1024	2048
1 A	248	224	197	153	132	84.9	85.3	36.4	14.3	10.8
2 A	180	184	170	157	131	116	70.8	44.4	73.6	56.7
3 A	46.2	43.4	40.0	40.8	43.0	42.8	38.5	40.1	79.0	49.0
4 A	70.3	88.4	84.6	81.5	75.2	55.9	30.6	25.2	48.9	24.4
5 A	129	81.6	57.9	34.7	17.5	20.2	14.1	11.9	11.1	10.9
6 A	416	279	208	129	98.0	81.7	54.1	36.4	21.9	26.5
7 A	157	176	199	254	207	99.5	66.2	52.2	68.1	92.3
8 A	105	124	120	123	82.1	85.5	85.1	30.4	32.8	11.2
9 A	75.4	79.5	83.1	80.2	78.1	57.2	48.8	31.6	33.6	121
10 A	24.1	25.9	26.2	21.7	17.3	8.74	9.15	2.70	33.5	187
11 A	112	117	140	144	126	93.5	59.8	39.6	61.3	96.4
12 A	41.0	92.6	81.6	67.3	64.4	47.0	92.5	120	272	2330
13 A	145	139	125	110	115	148	297	366	808	4430
14 A	110	123	107	76.3	53.1	42.1	41.6	43.1	66.7	298
15 A	146	137	116	66.3	49.3	31.6	45.9	24.6	59.9	180
16 A	348	279	224	146	85.2	54.8	49.6	22.1	82.7	235
17 A	248	186	153	104	68.6	55.7	37.4	22.5	12.7	9.28
18 A	246	181	151	105	73.8	58.4	38.6	22.4	28.6	89.6
19 A	259	195	151	96.6	64.6	48.4	33.9	23.2	20.9	7.35
20 A	850	542	394	244	149	95.5	42.7	20.7	14.5	54.0
21 A	1190	676	436	238	141	78.5	43.8	25.7	7.50	56.0
22 A	2820	1400	1050	547	293	145	50.1	45.2	123	406
23 A	2320	1180	816	480	328	249	307	126	105	122
24 A	573	259	149	70.4	58.1	54.4	54.4	64.1	91.6	82.4
25 A	438	255	173	101	58.6	47.5	33.0	15.1	23.3	10.8
26 A	71.6	72.9	70.7	64.8	61.7	44.7	28.1	33.7	52.1	163
27 A	65.0	80.4	86.9	91.3	86.7	80.5	55.5	44.1	19.7	8.78
28 A	134	140	141	126	113	74.0	45.8	27.9	22.0	26.8
29 A	125	123	119	99.6	95.0	64.6	70.9	44.5	25.7	508
30 A	131	122	139	162	190	178	157	146	129	79.4
31 A	333	326	307	241	251	178	142	77.7	34.5	128
32 A	95.1	89.1	86.8	82.0	73.1	44.9	26.3	29.8	39.8	101
33 A	169	132	111	81.3	59.9	33.0	17.0	12.9	14.3	21.4
34 A	180	180	156	148	132	125	153	114	522	1610
35 A	190	195	201	176	164	122	128	159	92.6	15.6
36 A	380	232	165	97.3	56.9	46.7	27.6	24.3	25.8	24.7
37 A	501	327	238	141	88.8	59.3	29.1	13.8	17.9	29.2
38 A	21800	17300	13200	8440	4950	5330	4470	2790	1930	671
39 A	121	92.7	77.1	50.7	42.6	44.2	28.2	22.2	14.8	8.41
40 A	747	516	432	316	237	241	221	140	105	122

unit : Ωm

List of Apparent Resistivity (2/8)

ST.NO. & DIPOLE	FREQUENCIES (HZ)									
	4	8	16	32	64	128	256	512	1024	2048
41 A	4890	2750	1950	1160	653	527	285	151	53.2	127
42 A	596	374	280	179	111	66.6	34.7	14.6	37.1	6.78
43 A	453	255	168	93.7	50.9	26.0	6.14	12.5	93.0	183
44 A	2120	750	461	290	174	162	153	67.9	13.4	5.32
45 A	893	358	191	112	94.1	78.4	77.1	50.4	86.2	55.0
46 A	559	208	116	62.0	61.5	54.1	57.9	21.4	137	219
47 A	425	209	108	47.1	39.6	42.5	46.6	42.8	57.8	106
48 A	522	340	258	163	107	87.4	58.9	36.1	36.5	44.4
49 A	301	219	176	126	101	83.7	75.7	55.7	39.4	32.0
50 A	105	120	125	114	92.3	73.1	114	26.8	21.7	68.3
51 A	43.0	48.7	75.1	88.5	83.8	73.9	36.3	23.8	11.6	3.58
52 A	281	358	431	469	513	445	272	156	63.5	38.5
53 A	428	487	548	515	451	312	182	93.3	34.1	6.29
54 A	268	263	224	166	127	73.0	99.9	87.2	179	69.2
55 A	641	633	785	616	511	295	422	491	518	507
56 A	800	1130	928	978	777	499	213	61.7	470	158
57 A	243	239	220	193	143	95.1	67.7	48.0	12.2	136
58 A	236	261	300	340	335	262	197	82.2	48.3	24.0
59 A	228	185	157	113	96.5	72.7	62.1	40.3	23.7	90.5
60 A	273	220	187	133	99.2	65.2	40.9	24.9	18.7	20.2
61 A	191	173	167	134	113	79.4	47.6	33.5	28.3	27.7
62 A	182	138	112	78.6	62.4	46.9	34.9	26.8	19.2	17.4
63 A	176	125	92.6	59.5	45.3	28.9	28.1	26.0	40.1	123
64 A	260	152	102	62.9	43.2	30.5	14.7	9.41	12.3	146
65 A	542	310	198	108	64.9	35.5	15.8	8.27	8.63	32.5
66 A	1600	869	564	313	183	91.4	52.1	34.0	20.6	5.68
67 A	137	80.0	57.3	31.6	20.0	10.9	10.6	11.3	9.14	11.7
68 A	139	137	129	97.9	78.3	52.1	30.3	18.0	8.15	21.3
69 A	16.1	7.63	5.25	3.95	5.52	7.04	8.88	9.52	5.66	6.30
70 A	33.1	36.4	38.3	40.8	36.4	28.8	22.2	32.7	75.8	109
71 A	15.8	19.6	19.9	18.5	15.7	13.3	11.5	9.64	6.40	3.92
72 A	20.9	21.2	22.0	19.2	17.6	14.2	19.1	18.8	7.45	46.2
73 A	61.4	79.3	60.9	54.8	35.1	26.8	10.4	3.72	1.84	20.4
74 A	265	222	170	93.3	74.5	42.6	150	250	475	3150
75 A	39.9	44.5	38.6	34.2	28.2	27.1	21.3	16.6	45.4	25.3
76 A	54.4	61.4	50.0	48.2	25.8	19.5	19.6	10.5	16.7	6.21
77 A	41.5	36.9	35.3	26.8	22.3	19.6	20.7	17.6	20.2	34.6
78 A	120	125	111	83.8	54.3	31.5	20.7	13.4	7.41	2.01
79 A	124	124	113	87.3	59.7	33.7	20.8	12.9	11.4	8.59
80 A	137	158	167	141	108	68.4	39.1	23.6	11.1	3.70

unit : Ωm

List of Apparent Resistivity (3/8)

ST.NO. & DIPOLE	FREQUENCIES (HZ)									
	4	8	16	32	64	128	256	512	1024	2048
81 A	106	118	151	157	134	100	70.5	34.6	19.9	31.9
82 A	495	629	769	847	964	898	604	512	399	181
83 A	134	144	168	166	155	109	72.4	40.7	20.5	12.6
84 A	67.6	88.3	104	98.4	95.3	57.8	51.0	25.3	17.1	7.80
85 A	148	194	229	245	257	221	138	61.9	62.7	21.9
86 A	59.1	70.0	74.8	74.8	62.0	46.6	24.3	15.4	6.44	4.33
87 A	108	119	120	107	81.5	56.5	29.6	17.9	11.3	4.17
88 A	112	107	108	88.2	64.0	37.7	20.6	22.0	7.25	23.7
89 A	167	132	95.7	64.3	35.0	20.8	15.0	13.7	10.9	7.25
90 A	296	242	213	149	87.2	48.4	25.0	15.9	10.9	7.49
91 A	267	241	167	118	63.8	33.2	21.7	14.0	14.2	52.7
92 A	422	322	252	165	94.7	51.7	30.9	19.0	20.1	45.8
93 A	114	98.5	90.0	77.0	64.0	38.9	17.4	5.77	20.2	27.7
94 A	283	209	181	110	88.9	52.2	22.0	10.5	28.5	15.6
95 A	197	130	108	76.5	51.0	37.6	43.5	36.6	15.4	82.7
96 A	250	201	179	128	84.3	48.5	29.1	25.4	18.0	31.6
97 A	465	335	264	183	113	70.0	52.3	48.0	55.6	51.7
98 A	583	345	241	154	96.3	54.8	33.8	47.4	46.3	41.3
99 A	2690	1290	719	457	344	209	138	121	144	179
100 A	3700	1370	734	506	357	247	153	130	115	119
101 A	498	154	87.2	63.9	43.8	40.3	36.8	46.4	54.2	58.7
102 A	1140	460	258	181	139	118	86.0	104	113	129
103 A	3120	1350	736	517	318	249	183	148	160	174
104 A	846	353	206	120	84.7	57.3	41.9	31.0	42.4	19.3
105 A	997	381	212	128	99.9	64.5	44.2	34.0	31.0	52.6
106 A	821	363	215	136	97.9	86.9	43.1	42.8	71.3	118
107 A	260	143	98.8	57.7	37.1	22.0	16.4	20.6	33.3	55.0
108 A	649	266	161	107	119	104	68.8	85.4	161	373
109 A	658	276	175	107	101	95.6	50.6	31.4	15.2	5.47
110 A	340	183	114	64.0	51.3	38.3	29.9	34.8	55.7	58.3
111 A	676	354	229	139	95.0	73.5	53.1	40.0	29.0	21.6
112 A	901	337	200	122	147	113	92.9	66.3	53.4	67.1
113 A	3480	1510	955	585	457	356	171	103	57.3	64.7
114 A	970	486	304	201	153	110	70.9	50.4	31.5	36.1
115 A	374	185	125	65.7	45.0	30.2	20.3	16.2	15.0	16.8
116 A	376	206	130	72.0	46.1	30.0	20.2	14.3	11.9	9.31
117 A	5550	2990	1800	1040	666	297	186	112	67.6	41.1
118 A	2480	1340	895	552	369	181	125	95.2	58.8	46.4
119 A	215	131	95.6	59.8	39.3	23.8	16.1	13.8	14.2	14.5
120 A	289	171	119	81.6	55.2	30.6	17.4	15.6	16.4	12.5

unit : Ωm

List of Apparent Resistivity (4/8)

ST.NO. & DIPOLE	FREQUENCIES (HZ)									
	4	8	16	32	64	128	256	512	1024	2048
121 A	444	309	250	173	136	76.9	45.1	31.8	19.1	17.5
122 A	184	134	106	84.3	68.8	44.0	26.4	14.8	8.42	8.23
123 A	850	419	244	141	71.2	54.7	34.1	31.8	35.6	44.3
124 A	924	436	260	137	75.7	53.3	43.6	42.0	53.9	92.1
125 A	186	101	71.7	46.4	29.3	23.6	20.1	18.3	18.7	22.7
126 A	323	172	111	63.0	35.5	24.0	19.4	17.6	16.4	13.5
127 A	288	159	111	65.1	37.4	19.0	15.6	16.2	16.8	14.2
128 A	175	100	72.8	45.9	26.7	16.7	15.6	17.4	18.5	17.4
129 A	290	142	102	67.2	44.2	38.4	33.2	33.1	39.2	36.1
130 A	418	192	120	84.1	48.5	33.1	29.4	38.2	43.2	46.7
131 A	227	70.0	50.0	41.4	21.3	16.9	21.2	23.0	32.5	36.7
132 A	255	177	183	120	91.6	64.8	42.6	27.7	19.3	16.4
133 A	314	216	160	105	97.3	80.8	63.7	44.4	26.0	14.9
134 A	1590	1140	941	730	715	545	418	351	245	208
135 A	77.1	94.0	94.2	98.1	71.9	59.5	42.2	22.7	14.6	14.5
136 A	633	507	451	341	256	126	67.7	35.7	23.1	19.4
137 A	342	262	238	184	135	73.2	37.7	22.3	14.9	12.0
138 A	109	113	124	122	104	71.4	43.6	29.9	24.8	22.2
139 A	378	320	333	287	185	114	59.6	33.3	20.3	12.0
140 A	671	456	336	219	108	58.7	55.2	52.9	46.4	18.5
141 A	141	93.8	67.8	44.6	27.5	18.4	19.1	23.1	26.2	19.8
142 A	149	186	226	253	256	206	132	87.2	55.8	37.1
143 A	177	221	271	331	412	452	361	243	168	105
144 A	572	279	164	101	101	79.1	75.3	74.2	70.3	51.2
145 A	729	322	190	111	104	97.7	90.3	80.7	69.1	55.5
146 A	1610	809	448	239	188	141	131	95.6	85.3	74.6
147 A	1920	833	456	268	193	122	88.7	63.7	49.6	63.4
148 A	58.8	55.4	54.8	51.2	45.5	38.1	32.7	25.4	30.7	39.0
149 A	11.0	13.6	12.4	15.2	23.4	37.7	37.2	18.1	9.38	27.2
150 B	456	303	259	384	453	470	395	371	400	88.3
151 B	96.1	77.7	77.5	88.4	89.0	75.6	83.5	57.8	56.8	8.31
152 B	195	187	175	170	169	109	73.5	35.5	20.1	17.5
153 B	249	132	59.4	39.4	43.7	27.4	17.1	10.6	8.82	5.01
154 B	1100	711	355	236	293	197	135	69.4	30.7	8.86
155 B	253	171	180	287	340	329	428	286	179	340
156 B	8890	6310	3990	3650	3800	2210	1200	1100	724	377
157 B	379	281	186	141	127	80.2	45.2	22.3	15.2	15.8
158 B	106	101	75.4	62.3	58.4	34.5	18.8	13.7	7.61	19.5
159 B	39.5	31.7	26.2	24.2	27.6	31.9	29.8	27.1	22.2	18.3

unit : Ωm

List of Apparent Resistivity (5/8)

ST.NO. & DIPOLE	FREQUENCIES (HZ)									
	4	8	16	32	64	128	256	512	1024	2048
160 B	38.5	32.9	25.8	23.3	28.8	32.6	41.6	27.4	18.7	21.3
161 B	107	102	98.7	92.2	80.0	64.4	49.0	30.0	24.9	26.2
162 B	33.1	28.8	24.4	20.9	17.8	12.6	9.64	6.42	4.47	4.48
163 B	22.7	24.1	24.0	30.7	33.8	34.4	41.9	25.8	24.0	21.6
164 B	29.7	25.9	23.8	30.4	34.8	32.3	81.7	45.0	47.8	48.7
165 B	194	141	78.6	47.0	42.4	22.7	12.4	11.0	10.6	10.8
166 B	327	195	101	46.5	43.4	23.5	14.3	9.51	7.45	6.93
167 B	1010	377	112	64.9	80.2	54.4	37.9	24.4	22.9	19.1
168 B	436	305	143	51.0	52.7	38.1	20.1	11.4	10.6	9.47
169 B	70.8	57.8	47.0	37.7	32.8	19.3	17.0	10.0	9.00	10.0
170 B	33.1	14.8	10.2	7.74	10.6	11.9	14.6	14.0	12.6	18.8
171 B	54.7	42.3	34.6	24.8	22.2	14.9	12.0	5.98	13.1	14.1
172 B	16.6	12.3	10.1	10.3	14.2	10.2	11.7	16.2	27.5	75.0
173 B	9.29	5.47	5.67	7.73	10.4	8.71	12.5	16.7	11.7	2.19
174 B	79.4	73.1	65.3	53.1	45.3	30.4	26.6	22.0	35.4	6.60
175 B	134	126	110	89.1	84.0	50.9	31.8	21.0	16.5	10.6
176 B	95.5	77.1	69.1	56.7	44.9	28.7	14.5	11.4	10.6	10.9
177 B	186	170	124	79.0	86.4	56.9	25.2	15.3	10.0	11.3
178 B	134	108	87.3	64.2	57.0	37.3	20.1	10.5	13.7	4.00
179 B	204	183	130	97.6	86.1	65.9	31.8	18.4	26.8	77.9
180 B	120	96.7	91.5	66.9	57.8	39.0	24.7	12.8	8.95	9.63
181 B	76.8	72.2	59.9	51.7	60.0	27.5	13.6	10.6	8.26	6.94
182 B	184	180	150	153	121	85.5	47.4	25.9	18.2	14.6
183 B	101	90.3	80.9	65.9	54.8	25.3	15.7	13.4	10.8	6.96
184 B	207	171	118	65.1	58.6	33.3	19.4	12.7	11.5	11.9
185 B	357	284	187	84.0	74.6	43.5	21.5	12.2	7.59	7.83
186 B	491	375	226	93.0	83.7	43.7	27.4	13.0	19.5	6.23
187 B	133	110	80.9	45.3	43.4	25.8	14.9	9.56	7.93	7.41
188 B	1120	1060	1070	992	920	569	413	255	172	132
189 B	173	158	142	114	111	60.5	40.5	22.0	11.1	10.5
190 B	110	121	89.3	37.1	29.9	20.6	12.5	8.56	7.95	8.80
191 B	178	132	82.2	33.5	22.1	14.6	7.35	6.13	7.53	7.45
192 B	487	328	192	85.4	40.5	28.6	18.0	11.9	9.26	8.22
193 B	461	254	137	55.4	28.5	17.1	9.99	9.65	8.78	9.29
194 B	550	325	173	68.7	26.7	19.4	12.1	10.3	9.63	12.2
195 B	907	537	270	95.9	39.9	30.0	18.1	11.2	8.63	7.60
196 B	452	295	157	58.6	35.0	26.8	14.5	10.7	9.57	10.7
197 B	492	353	214	82.9	63.5	39.5	20.2	11.5	12.7	14.2
198 B	728	496	276	100	63.7	47.3	28.5	17.9	11.8	10.8
199 B	802	560	313	111	89.0	58.4	33.7	20.9	13.9	14.5

unit : Ωm

List of Apparent Resistivity (6/8)

ST.NO. & DIPOLE	FREQUENCIES (HZ)									
	4	8	16	32	64	128	256	512	1024	2048
200 B	754	391	182	65.9	72.1	44.6	23.5	15.3	12.5	11.0
201 B	1360	907	495	174	143	116	83.2	48.0	29.7	22.0
202 B	1040	684	350	121	90.6	70.5	42.3	26.7	19.3	9.59
203 B	845	546	308	112	68.2	50.6	29.2	18.3	13.8	11.5
204 B	801	480	254	85.4	48.0	36.7	22.3	17.2	15.5	14.9
205 B	590	331	169	62.3	25.4	17.9	11.1	75.4	6.55	8.17
206 B	1160	830	481	189	190	142	89.2	53.1	30.2	27.8
207 B	493	271	141	77.8	82.5	52.9	28.0	15.3	9.27	25.2
208 B	1010	618	306	151	169	109	45.7	29.6	20.9	14.8
209 B	296	218	132	84.2	83.2	55.8	26.8	15.3	9.17	16.6
210 B	899	588	309	129	123	80.2	39.3	24.9	16.9	14.9
211 B	1740	1060	494	215	235	157	139	121	91.8	48.5
212 B	1100	519	202	127	155	120	62.9	37.2	28.2	27.5
213 B	412	278	151	69.6	64.5	35.0	22.2	11.8	10.8	9.30
214 B	211	139	90.8	105	117	80.8	84.1	45.4	17.2	6.47
215 B	4460	2510	1730	2420	2940	3080	2840	1980	1720	769
216 B	60.4	45.2	49.6	60.9	66.3	67.5	76.1	43.0	23.7	11.8
217 B	67.9	34.1	30.9	34.6	26.5	27.5	25.5	14.9	18.0	38.6
218 B	70.6	32.3	22.0	25.7	29.4	73.0	99.9	85.8	85.8	48.2
219 B	577	482	210	245	331	477	581	412	334	201
220 B	1360	726	385	219	248	184	117	77.3	60.8	50.5
221 B	141	117	80.1	56.8	52.0	29.5	19.2	15.6	15.7	24.4
222 B	3360	1730	884	452	370	234	123	73.7	58.3	50.8
223 B	335	322	267	190	180	134	80.5	39.8	23.9	12.8
224 B	397	449	307	204	156	91.1	44.7	22.4	12.6	9.48
225 B	941	612	357	181	104	70.1	37.9	26.5	21.5	24.6
226 C	356	321	345	285	208	134	74.6	54.3	63.8	58.0
227 C	117	89.2	140	116	108	109	103	55.8	14.6	29.5
228 C	33.3	39.0	41.9	36.8	43.2	32.6	24.1	14.4	7.65	3.24
229 C	70.7	50.1	56.9	55.5	63.4	66.4	60.1	40.7	30.0	21.9
230 C	46.5	75.9	117	106	76.0	61.6	37.5	22.2	13.6	5.46
231 C	544	708	1040	1270	1350	1250	948	681	447	215
232 C	52.9	71.7	110	121	124	94.8	78.1	61.0	43.9	37.8
233 C	55.8	69.7	107	129	158	118	113	101	79.0	95.3
234 C	29.3	25.0	31.3	41.3	51.5	50.0	50.1	37.2	30.3	51.9
235 C	590	519	495	500	474	314	171	88.7	51.6	37.1
236 C	156	141	132	134	149	130	86.6	60.3	32.4	33.4
237 C	1040	967	872	873	634	304	153	67.2	33.8	36.7
238 C	88.4	122	190	283	276	162	67.9	36.2	23.2	23.3

unit : Ωm

List of Apparent Resistivity (7/8)

ST.NO. & DIPOLE	FREQUENCIES (HZ)									
	4	8	16	32	64	128	256	512	1024	2048
239 C	705	750	862	884	743	404	204	97.5	46.9	21.5
240 C	97.8	90.0	130	128	107	51.8	34.3	15.5	14.4	30.8
241 C	160	182	162	112	61.3	37.4	20.5	9.64	5.42	4.14
242 C	675	1110	1660	1350	839	393	217	84.1	32.1	106
243 C	129	192	190	150	107	61.6	31.7	11.7	14.9	127
244 C	192	205	266	377	493	403	210	70.9	21.5	92.4
245 C	664	928	1360	1760	2500	2190	1100	575	400	326
246 C	164	198	251	297	321	236	143	73.3	46.5	17.7
247 C	206	310	484	657	827	640	367	196	101	73.4
248 C	423	552	595	690	734	539	310	183	111	55.8
249 C	88.4	101	134	137	148	127	95.1	65.5	34.7	74.0
250 C	250	269	305	264	171	93.6	51.5	28.2	31.1	61.5
251 C	286	277	287	231	163	84.1	41.6	17.9	12.7	7.14
252 C	358	339	386	327	239	143	68.8	39.8	30.3	40.1
253 C	331	320	448	457	397	289	157	100	125	335
254 C	4360	4570	5350	5110	4700	3400	2240	1390	874	698
255 C	52.8	77.4	119	146	195	231	258	259	166	106
256 C	9250	8910	12300	10800	11000	7740	6180	5460	5530	1710
257 C	106	142	203	230	257	292	356	394	344	348
258 C	704	809	1110	1390	1200	1110	1010	923	512	1120
259 C	1420	1660	2070	2020	1590	1140	795	600	339	572
260 C	132	140	121	68.7	47.0	55.3	66.4	56.1	44.6	44.5
261 C	420	444	443	290	166	166	168	140	121	130
262 C	150	172	197	183	211	258	297	316	282	147
263 C	2450	2110	2310	2370	1960	1410	740	432	262	235
264 C	337	335	352	419	300	209	125	65.6	34.0	15.9
265 C	553	595	641	639	525	409	308	202	94.3	27.0
266 C	641	636	623	500	340	256	179	119	64.8	29.1
267 C	71.4	66.4	43.9	13.1	32.8	70.4	89.6	89.2	93.1	57.8
268 C	301	289	339	334	324	243	165	92.0	48.4	10.8
269 C	443	460	527	603	572	452	317	179	80.0	48.1
270 C	686	654	708	708	726	797	726	630	406	353
271 C	272	264	292	315	390	462	563	521	340	389
272 C	548	517	634	536	410	247	129	58.7	33.5	29.7
273 C	532	467	540	551	457	302	179	84.9	38.6	20.1
274 C	342	289	326	308	257	141	71.5	35.7	23.2	23.3
275 C	142	134	141	139	115	84.3	55.6	32.4	26.3	36.4
276 C	391	361	381	391	403	368	290	207	133	99.5
277 C	4520	3860	3900	4100	4160	3780	3630	3280	2320	545
278 C	5910	5300	5430	5710	5540	4330	3150	2330	1530	1000

unit : Ωm

List of Apparent Resistivity (8/8)

ST.NO. & DIPOLE	FREQUENCIES (HZ)									
	4	8	16	32	64	128	256	512	1024	2048
279 C	2370	2190	2410	2660	2790	2350	2080	1940	1690	1320
280 C	10400	8670	8780	8130	8330	7460	7300	6220	4390	3240
281 C	2920	2600	2600	2730	2530	2340	2210	1840	1290	908
282 C	955	856	890	849	890	743	604	435	270	165
283 C	340	317	321	322	301	215	151	86.0	43.6	29.0
284 C	354	272	275	258	220	142	81.7	43.0	20.8	36.0
285 C	899	698	669	636	563	412	250	149	80.4	20.5
286 C	753	565	558	514	425	284	169	90.7	39.9	14.3
287 C	3780	3120	3200	3290	3400	2820	2380	1560	891	261
288 C	7030	6110	6530	6890	7120	6260	5830	3640	1330	216
289 C	3960	3690	3820	4020	4100	3060	2000	1150	524	134
290 C	832	771	786	805	772	572	406	247	103	38.4
291 C	1370	1300	1410	1510	1530	1250	898	616	364	199
292 C	1300	1150	1280	1450	1490	1100	649	328	144	65.7
293 C	822	926	1200	1390	1420	965	523	241	109	53.7
294 C	1370	1460	1690	1930	1900	1130	776	351	187	133
295 C	298	319	416	506	578	478	337	224	138	104
296 C	1200	978	1040	1130	1090	780	522	312	220	64.3
297 C	880	728	726	805	779	577	372	225	157	61.1
298 C	1450	1090	1240	1290	1170	919	527	325	103	91.0
299 C	539	394	375	376	378	277	157	84.5	53.7	43.0
300 C	312	321	397	459	498	367	217	136	79.1	43.6
301 C	1090	1290	1510	1430	1290	782	411	226	122	34.7
302 C	253	216	382	592	931	761	566	364	263	88.8

unit : Ωm

CHAPTER 2 RESULT OF THE SURVEY

Results of laboratory test of physical properties on rock samples, apparent resistivity measurement, and one dimensional inversion of all CSAMT measurement were illustrated in the following figures:

Tab. II-2	Rock Properties
PL. II-2 to II-11	Apparent Resistivity Map
Fig. II-10 to II-17	Apparent Resistivity Pseudo-Section with Estimated Resistivity Structure
PL. II-12 to II-15	Resistivity Structure Map

In the following sections, the above mentioned figures are explained.

2-1 Physical Properties of Rock Samples

Twenty-four samples of representative rocks from the survey area are tested in laboratory for their resistivity, density, and magnetic susceptibility. The results are shown in Tab. II-2.

Characteristics of rock properties are as follows:

i) Geometric average of resistivities of rock samples are clearly divided into the following three groups.

	Formation	No. of samples	Average
Low Resistivity	Ore of Hajar mine	4	15 Ω m
Medium Resistivity	Quaternary	2	57 Ω m
High Resistivity	Carboniferous to Permian	18	500 Ω m
All samples		24	230 Ω m

ii) Except ore samples from Hajar mine, which have very low resistivity, resistivity structure in the survey area consists by a resistive basement of the Permian to the Carboniferous and a overlying medium to low resistivity layer of the Quaternary. The Quaternary including some Pliocene is an aquifer with a free ground water table.

iii) Density of rock samples is also divided into two groups, high density basement of the Permian to the Carboniferous and low density overlying layer of the Quaternary. Ore of Hajar Mine has distinctively high density.

iv) All rock samples except ore samples have low magnetic susceptibility. Magnetic susceptibility of ore samples from Hajar mine is extremely high and magnetic survey for ore must be very effective.

2-2 Apparent Resistivity Map (see PL. II-2 to II-11 and Fig. II-5 to II-9)

Apparent resistivity is not the same as true formation resistivity but qualitatively reflects underground resistivity structure. Apparent resistivity reflects resistivity structure of relatively shallow structure for higher frequency and it of lower frequency reflects deeper structure.

Apparent resistivity values are divided into the following five groups.

10Ω m	40Ω m	250Ω m	1000Ω m	
very low app. resistivity	low app. resistivity	medium app. resistivity	high app. resistivity	very high app. resistivity

We studied all apparent resistivity data about static shift which is an erroneous shift of apparent resistivity vs. frequency curves only along the vertical axis, namely the resistivity axis, caused by local inhomogeneity at or near the ground surface. As a result, apparent resistivity data of the stations 38, 156, and 188 are obviously shifted to higher resistivity in the entire frequency range. Therefore the data from those three stations are eliminated from the interpretation.

(1) General View of Apparent Resistivity Distribution

General view of apparent resistivity distribution of ten frequencies, from 4 Hz to 2,048 Hz, is summarized as follows:

i) Generally, apparent resistivity is tend to be low in higher frequency and high in lower frequency. This tendency is remarkable in the center and the eastern part of the survey area.

ii) Arrangement and its direction of apparent resistivity anomalies are dominantly in NW-SE direction in lower frequency, and this directionality disappears in higher frequency.

iii) Apparent resistivity distribution has the following characteristics:

Eastern part	Generally small apparent resistivity anomalies are seen. Anomalies tend to aline in NW-SE direction.
Central part	Apparent resistivity value varies gently and very low apparent resistivity anomalies are seen in high frequency.
Western part	Apparent resistivity does not vary so much and high apparent resistivity is dominant in all frequency.

(2) Apparent Resistivity Distribution of Individual Frequency

The apparent resistivity distributions of five frequencies, 4 Hz, 16 Hz, 64 Hz, 256 Hz, 1,024 Hz, are explained in the following section.

i) Apparent resistivity map in 4 Hz (see PL. II-2 and Fig. II-5)

High apparent resistivity covers most of the area except around Taguennza and the southwest of Barrage Cavagnac where low apparent resistivity zones are. High apparent resistivity zones are arranged in NW-SE lines, from Tiouli to Hajar mine, from northeast of Souksou to Amzourh, and from Mkhalif to Arissa. The arrangement of high apparent resistivity zones may show existence of resistive basement.

Hajar mine is at the center of a high apparent resistivity zone and is located between two very high apparent resistivity zones, in its northwest and its south.

ii) Apparent resistivity map in 16 Hz (see PL. II-4 and Fig. II-6)

Apparent resistivity distribution in 16 Hz shows no significant change but slightly lower resistivity in the eastern half of the survey area in comparison with it in 4 Hz.

It indicates a characteristic feature of apparent resistivity distribution around Hajar mine that Hajar mine is surrounded by three high apparent resistivity zones.

iii) Apparent resistivity map in 64 Hz (see PL. II-6 and Fig. II-7)

Apparent resistivity distribution in 64 Hz shows lower resistivity at around Hajar mine and Souksou in comparison with it in 16 Hz. High apparent resistivity zone appears near Amzourh in NW-SE direction.

iv) Apparent resistivity map in 256 Hz (see PL. II-8 and Fig. II-8)

High apparent resistivity area decreases and low apparent resistivity area increases largely at near Souksou and the west of Hajar mine. In the south of Oukhribane, high apparent resistivity zones and low apparent resistivity zones are arranged side by side in NW-SE direction.

v) Apparent resistivity map in 1,024 Hz (see PL. II-10 and Fig. II-9)

High apparent resistivity zone shrinks in comparison with in 256 Hz. Very low resistivity zone is dominant in the central part of the survey area.

Many small medium apparent resistivity zones are in between Amzourh and Akhlij and the entire area is surrounded by low apparent resistivity area.

The area around Hajar mine does not outstand in apparent resistivity distribution in 1,024 Hz not like in other frequencies.

2-3 Apparent Resistivity Pseudo-Section and Estimated Resistivity Structure (see Fig. II-10 to Fig. II-17)

The sections of A-A' and B-B' cut the eastern part of the survey area in NNW-SSE direction. The sections of C-C', D-D', E-E' and F-F' cut the central and the eastern part of the survey area in WSW-ENE direction. The sections of G-G' and H-H' cut the western part of the survey area in E-W direction. In each map, an apparent resistivity section and a resistivity structure section are illustrated.

Resistivity values are divided into as follows, not the same as apparent resistivity division:

40Ωm		150Ωm	1000Ωm	4000Ωm
very low resistivity	low resistivity	medium resistivity	high resistivity	very high resistivity

(1) A-A' section (Fig. II-10)

This section runs NNW-SSE direction over Hajar mine.

The apparent resistivity section shows low to medium apparent resistivity in higher frequencies but in lower frequencies apparent resistivity drastically changes into high, about 1,000Ωm. Low apparent resistivity anomalies surrounded by a contour line of 65Ωm are found at near Hajar mine, the stations 43 and 67 in the frequencies between 256 Hz and 1,024 Hz.

The resistivity section consists by two to three layers with the resistive basement except at near the ground surface. Depth to the resistive basement is shallow, about 100m in the center and the north of the section and very deep, about 1,000 m and forms a concave at around Hajar mine.

Hajar ore deposit is at a concavity of the resistive basement, has medium resistivity of about 200Ωm, and is controlled its both ends by resistivity discontinuity. Extremely low resistivity which may directly indicate ore was not found around Hajar mine. Instead, mineralization of Hajar mine is found as a low resistivity anomaly in the basement which may be seen as a concavity of the basement in the resistivity section.

(2) B-B' Section (see Fig. II-11)

Apparent resistivity in the section tends to increase its value toward lower frequencies. Higher apparent resistivity zone and lower apparent resistivity zone appear alternatively in horizontal direction.

The resistivity section consists by three layers in general, but is controlled by resistivity discontinuities, and varies horizontally. At the center of the section the resistive basement is shallow and contains relatively lower resistivity part deep in the ground. Resistivity value varies in the resistive basement.

Concavities of the basement are found at the stations 3, 165, and 167, near Lamrah and the station 55 in the south of the section.

(3) C-C' Section (see Fig. II-12)

The section C-C' cuts through Hajar mine.

The apparent resistivity section shows similar apparent resistivity distribution as the section A-A' but with some lower apparent resistivity values.

The resistivity section consists by two to three layers with some variation in apparent resistivity which may be caused by influence of an underground water table. The resistive basement is shallow at the center of the section and is not seen in the west end of the section, the stations between 14 and 77, because the near surface conductive layer is very thick and the CSAMT survey could not reach the resistive basement.

Small concave of the resistive basement is seen at near Hajar mine and the station 54.

(4) D-D' Section (see Fig. II-13)

The apparent resistivity section shows very low apparent resistivity in the west end of the section and that apparent resistivity values generally increase to east with some variations and become high at the east end of the section, the station 41.

The resistivity section consists by three layers in the center and the west of the section. Along the section, layers are arranged the low resistivity layer at the top, the resistive basement, and the low resistivity part of the basement at the bottom. The bottom low resistivity layer is assumed to be a conductive part in the resistive basement and located in the depth of the area between the stations 62 and 19. The geological structure in the area generally declines toward the west and consists of some different resistivity layers alternatively. Resistivity structure in the west of the discontinuity is rather different and the resistive basement was not detected as the section C-C'.

(5) E-E' Section (see Fig. II-14)

The apparent resistivity distribution in the section shows high resistivity at the center of the section and low at the both ends. Very conductive zone is found at the station 69. The resistivity distribution shows discontinuity at between the stations 153 and 211.

The resistivity section consists by two layers in the west end and changes into three to four layers at the east end of the section except layers near the surface of the ground. In the east of the section, the resistive basement shows upheaval centered at the station 216 and declines toward the west. A high resistivity layer is also found at near the ground surface of the center of the section, but low to medium resistivity layers are dominant under the shallow resistive layer.

The resistive basement may upheave at the shallow part around the stations 153 to 211 from the resistivity section of B-B'.

(6) F-F' Section (see Fig. II-15)

The apparent resistivity section shows relatively linear increase of apparent resistivity from 10 Ωm of high frequency to 1,000 Ωm of low frequency. Apparent resistivity distribution varies little by the stations.

The resistivity structure in the section is generally three layers. At the west of the section, the resistive basement is at shallow depth with variation of resistivity value. In the resistive basement, relatively low resistivity layer is found at deep in the ground. At the east of the section, resistivity structure consists of a very conductive layer at the top, a medium resistivity layer at the second and a resistive base at the bottom. A concavity of the resistive basement is assumed at around the stations 201 and 202.

(7) G-G' Section (see Fig. II-16)

The apparent resistivity distribution in the section shows that apparent resistivity increases from low frequency to high frequency and very high apparent resistivity in all frequencies are seen at the stations 254 and 287. An apparent resistivity discontinuity is between the stations 253 and 254.